Worcester Polytechnic Institute
Digital WPI

Major Qualifying Projects (All Years) | Major Qualifying Projects

April 2011

StandAlone Surgical Haptic Arm (SASHA)

Andrew Walker Lewis
Worcester Polytechnic Institute

Daniel Tice Jones
Worcester Polytechnic Institute

Follow this and additional works at: https://digitalcommons.wpi.edu/mqp-all

Repository Citation
Lewis, A. W., & Jones, D. T. (2011). *StandAlone Surgical Haptic Arm (SASHA)*. Retrieved from https://digitalcommons.wpi.edu/mqp-all/105

This Unrestricted is brought to you for free and open access by the Major Qualifying Projects at Digital WPI. It has been accepted for inclusion in Major Qualifying Projects (All Years) by an authorized administrator of Digital WPI. For more information, please contact digitalwpi@wpi.edu.

STANDALONE SURGICAL HAPTIC ARM (SASHA)

A Major Qualifying Project Report

Submitted to the faculty of

WORCESTER POLYTECHNIC INSTITUTE

In partial fulfillment of the requirements for the

Degree of Bachelor of Science

By:

Daniel Jones

Andrew Lewis

Advisors:

Professor Gregory Fischer

Professor Taskin Padir

4/28/2011

Abstract

A standalone surgical arm for performing Minimally Invasive Robotic Surgery (MIRS) with standard da Vinci Si tools has been developed. Force feedback is now possible with the feedback from torque sensors used to measure the forces acting upon the tool tip. The mechanical arm and a control system capable of driving the arm and reporting force information to the user via haptic feedback has been designed and fabricated. This arm will be used as a platform for research on the performance of telesurgery as a function of various haptic mappings and artificial latencies.

Acknowledgements

The group would like to thank Professor Gregory Fischer, Professor Taskin Padir, Michael Fagan, and Neil Whitehouse for their assistance with the realization of this project.

Additional thanks go to Comprehensive Power Inc. for their generous motor and power supply donations; igus for the generous donations of many of their products; and Allen Medical for their indispensible donation of operating table clamps. Special thanks to Boston Children's Hospital for their advice and support.

Contents

List of Figures

List of Tables

Introduction

Executive Summary

Minimally Invasive Robotic Surgery (MIRS) is a relatively new method of performing surgeries which uses surgical robots to perform laparoscopic surgery. This has several advantages over using traditional laparoscopic tools, as the manipulators can have many more degrees of freedom and more natural motions can be used by the surgeon to control the robot. Current commercially available MIRS systems such as the da Vinci from intuitive Surgical do not provide force feedback to the surgeon, so the surgeon cannot feel how much force he is applying to different tissues or is using in tying a suture.

A previous MQP developed a method of sensing the forces used in manipulating one of the da Vinci tools (Marchese & Hoyt, 2010). This was accomplished by placing a module between the tool and the da Vinci manipulator. This module contains aluminum couplers with strain gauges to measure the torque applied to each of the tools degrees of freedom.

The goal of this project was to construct a surgical arm that would be suitable for use in research into haptics and telesurgery. It should allow for forces to be reported back and for the mapping and timing of those forces to be reported back to the surgeon in various ways. It should also be possible to experiment with varying artificial delay times when performing telesurgery.

The arm was designed to maintain a remote center of motion through mechanically constrained links. A tool interface and carriage was designed to interface directly with a standard da Vinci Si faceplate. This interface also includes motor modules to drive the tool tip and torque sensors for measuring each Degree of Freedom (DoF) of the tool tip. The linear slide assembly is manipulated by a 2 rotational DoF arm that mechanically couples opposing links to remain parallel to each other. The arm is supported by a passive positioning system that allows for positioning of the remote center in 4 DoF.

To control this arm, a control system comprised of multiple motor controllers and a torque sensor interface talking to a master kinematics controller was devised. Two different sizes of motor controllers were designed and fabricated for the two different types of motors, and a strain gauge interface board was also designed and manufactured. These communicate back to the master kinematics controller, which is a Java program running on a PC. The master kinematics controller controls the overall position of the arm and tool tip through its commands to the motor controller boards. It also maps the forces reported back by the motor controllers and strain gauge interface to the user.

Some additional work will be required to bring this arm to the point where it will be usable for research. The main limitation to the mechanical system is the inability of the timing belt system to support the cantilevered weight of the robot. This can be easily fixed by replacing the timing belts with a chain and sprocket system. The software on the motor controllers and the kinematics controller is still mostly incomplete and needs to be expanded to allow for additional control modes and more configurability and feedback information. The kinematics controller should then be interfaced to the PHANTOM Desktop from Sensable so that the arm can be manipulated with force feedback.

Literature Review

The two most common modern techniques for performing surgery are open surgery and Minimally Invasive Surgery (MIS). Open surgery is performed through a large incision through which the surgeon can see and manipulate the afflicted area, whereas minimally invasive surgery is performed with specialized tools and cameras that are inserted into the body through small keyholes as seen in Figure 1. (Parker, 2010). MIS is commonly chosen over open surgery because of the reduced recovery time and decreased physical scarring. Furthermore, MIS is often less expensive than open surgery because shorter recovery times lead to shorter stays in the hospital, which can be a significant portion of the cost of surgery. Laparoscopic surgery is a type of minimally invasive surgery that is used to operate primarily in the abdominal region because of the easy access and open space available to maneuver the tools.

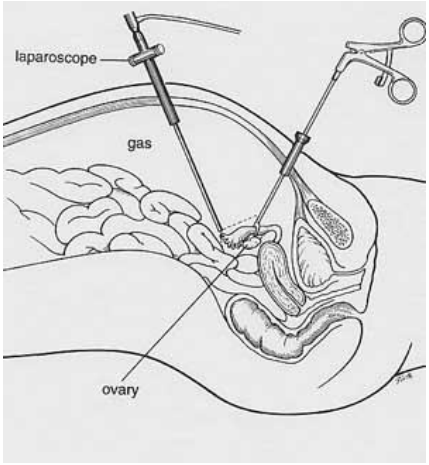

Figure 1: Diagram of Laparoscopic Minimally Invasive Surgery

During the 1990's a new form of MIS was commercially introduced: laparoscopic surgery aided by robotic manipulation. Minimally Invasive Robotic Surgery (MIRS) is currently dominated by Intuitive Surgical's da Vinci system seen in Figure 2. (Intuitive Surgical, 2010) The first da Vinci system was introduced in 1999, and the most recent da Vinci SI system offers a 3D HD vision system, three robotic arms with surgical tools and another robotic arm for controlling an endoscopic camera (Intuitive Surgical, 2010). All of the arms attach to a common column that is wheeled to the operating table prior to surgery. A wide variety of interchangeable and disposable tools allows for a wide variety of surgical procedures that would be impossible to perform with traditional laparoscopy.

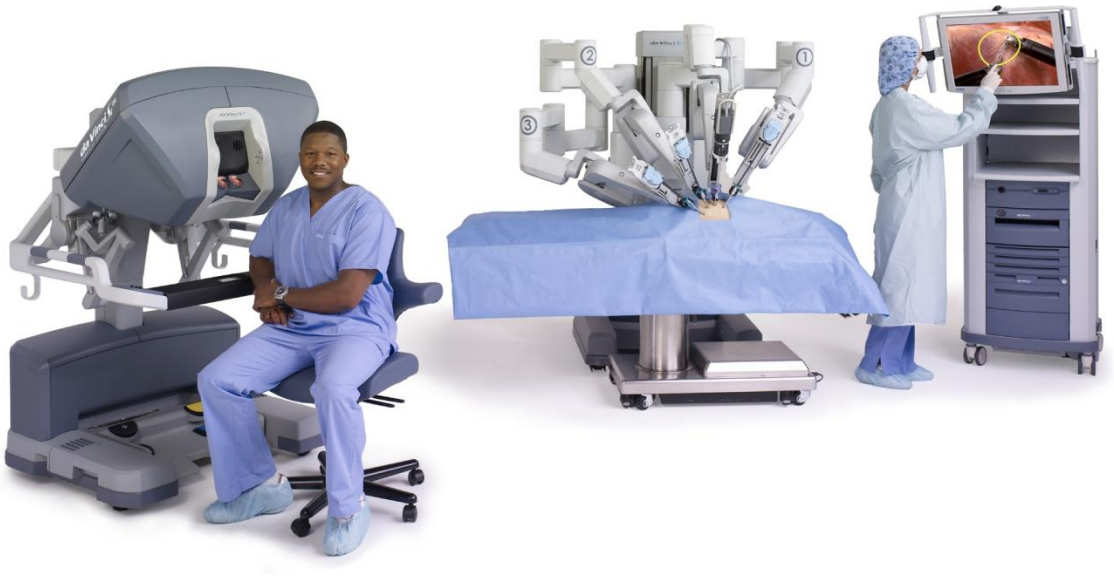

Figure 2: Intuitive Surgical's da Vinci Si Surgical System

A significant advantage to using the da Vinci system is that instead of spending the entire surgery standing next to the patient, a surgeon using the da Vinci surgeon controls the surgery from a seated position separated from the patient. This method of performing surgery distanced from the patient is known as telesurgery and can theoretically be performed from any distance. The capabilities and limitations of telesurgery has been an area of great interest to many researchers.

Another area of interest to researchers is the use and effects of haptics in telesurgery. Haptics is the representation or replication of physical or virtual forces upon a user controlling a system. This representation can range from the simple vibration feature common in modern video game systems to the advanced 7 Degree of Freedom (DoF) haptic controllers available from Force Dimension (Figure 3) (Force Dimension, 2011). When operating traditional laparoscopic tools, the surgeon is able to directly feel how much force is being applied, which is untrue of commercially available MIRS systems. However, several robotic surgical systems are being developed to make use of emerging haptic technologies and will be explained later.

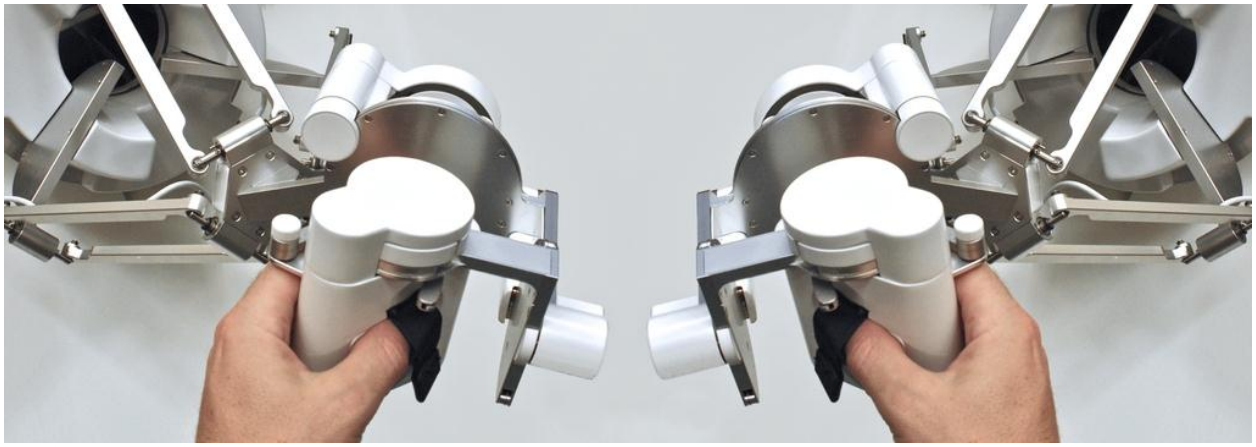

Figure 3: Force Dimension Haptic Controller

Telesurgery

Before 2001, it was believed that long distance telesurgery would be limited to telementoring from within a few hundred miles of the surgery (Marescaux, et al., 2001). Researchers experimented with robot assisted laparoscopic removal of pigs' gallbladders where the surgeons were located in Strasbourg, France and the pigs were located in Paris, a distance of around 1000 kilometers. The time difference between the surgeons' motions to the corresponding motion on the surgeon's video feed was about 20 ms, but the researchers experimented with artificially creating lag times of up to 551.5 milliseconds. According to the perceptions of the surgeons, the maximum, safe time lag was determined to be around 330 milliseconds. The researchers then performed this experiment between New York and Strasbourg, a distance of greater than 14000 km round trip. The researchers were able to obtain a dedicated fiber optic connection with a bandwidth of 10 megabits per second with a Network Termination Unit. It was found that with Asynchronous Transfer Mode (ATM) they were able to receive every packet of information that was between the stations without error. The time lag between France and the US was about 78 to 80 milliseconds without the 70 ms lag due to coding and decoding the video. The total lag, with the addition of a few milliseconds lag due to converting between Ethernet and ATM, was about 155 milliseconds between a surgeon's initial movements and the corresponding movements on his screen. Marescaux and the other surgeons were highly confident in the results of the experimental surgeries and successfully performed the first transatlantic telesurgery on a 68 year-old female who was discharged 48 hours after the groundbreaking surgery.

The use of telesurgery and telementoring has grown in Canada since the first transatlantic telesurgery, sometimes known as "Operation Lindbergh." Dr. Anvari at St Joseph's hospital in Hamilton, Ontario regularly performs telesurgeries in North Bay General Hospital, located in a rural community 400 km away (Kay, 2004). Dr. Anvari also telementors less experienced surgeons from his hospital in Hamilton. The use of telesurgery is still experimental and expensive, but many hope that someday it will be comparable in cost to transporting patients from rural locations to larger communities. This is especially helpful in Canada, where there are 10 million people living in rural or sparsely populated areas. Due to the high cost of dedicated fiber, Dr. Anvari's hospital uses common fiber with a Virtual Private Network (VPN) to ensure that data is not lost. Bell Canada is also researching fiber optic and satellite

communication solutions so that telesurgery can be used effectively in war-zones. The Canadian Space Agency and NASA are working with Dr. Anvari and Bell Canada towards the goal of being able to use telesurgery on the international space station. Dr. Richard Satava predicts that all surgeries will be automated within 40 to 50 years.

Surgical Robotics Research

The majority of Radical Prostatectomy surgeries performed in the US are robot assisted due to the introduction of the da Vinci surgical system. This procedure is known as Robot Assisted Laparoscopic Radical Prostatectomy (RALRP). LRP was first performed in 1992 in the US, but it was deemed "too difficult" and was not pursued any further, although European surgeons continued to develop the procedure. The widespread use of LRP and the economic conditions in Europe have kept the use of RALRP from spreading as quickly as in the US. (Murphy, Challacombe, & Costello, 2008)

There is minimal randomized evidence to confirm that RALRP is significantly better than Open Radical Prostatectomy (ORP), however many surgeons believe that RALRP is easier and better for the patient (Murphy, Challacombe, & Costello, 2008). RALRP is inherently minimally invasive, and there is evidence that shows that RALRP performs better in terms of blood loss, transfusion requirements, post-operative pain and hospitalization time. Not only are these benefits inherently positive, they also lead to an overall lower cost of surgery. Murphy et al. conclude that although there lacks randomized evidence to confirm that RALRP is better than ORP, it is at least as good as ORP and has already cemented its place in radical prostatectomy.

Nine out of 350 (2.6%) RALRPs were unable to be robotically assisted at Virginia Mason Medical Center due to failure of the da Vinci system (Borden, Kozlowski, Porter, & Corman, 2007). Six of these failures were detected before surgery and the surgeries were postponed. The other 3 malfunctions occurred during surgery but did not result in patient harm. Five of the malfunctions were mechanical malfunctions, 3 were electrical challenges and one was due to software incompatibility. The research concluded that although rare, robotic malfunctions can lead to psychological, financial and logistical burdens for patients, physicians and hospitals.

John's Hopkins University conducted a study into suturing comparing the forces involved in suturing by hand, by instrument, and by robot, and comparing the differences between experts and novices in each of these (Kitagawa, Okamura, Bethea, Gott, & Baumgartner, 2002). The robot used for this study did not have force feedback, and it was found that for traditional instrument ties there were slightly better forces then for the robot ties. It was also found that using traditional instrument ties provided more consistent forces than robot ties, suggesting that force feedback in a robot could improve repeatability. It was also found that the difference between the experts and novices for both the instrument and robot ties were much smaller than for the hand ties.

The Iwate University has created an attachment for the da Vinci robot arm which allows it to sense forces in its tool (Shimachi, Hirunyanitiwatna, Fujiwara, Hashimoto, & Hakozaki, 2008). This was done be constructing a device which the standard da Vinci tool interfaces with. The shaft of the tool is encompassed by an overcoat pipe with force sensors along it, allowing for forces to be sensed in the

along the shaft and perpendicular to it. This system would allow for force feedback to be provided to the surgeon using the da Vinci.

The Institute of Robotics and Mechatronics in Germany is developing a set of forceps with integrated actuation and force sensing (Kuebler, Seibold, & Hirzinger, 2005). This uses force transducers in structure called a Stewart Platform in the tip of the forceps. This allows for the forces to be measured directly where they are being applied. This would provide a surgical tool with force sensing measured directly where the tool is acting, thus providing the user interface with the information it needs to provide the user with accurate force feedback. This system has been designed and constructed and is currently being tested.

Alternate Robotic Surgical Systems

Following the da Vinci's widespread success, there is a variety of research being performed to develop new MIRS systems. The German Aerospace Center (DLR) has developed its second generation robotic arm (MIRO) that is used in its MiroSurge robotic system (Figure 4) (Institute of Robotics and Mechatronics, 2010). The arms weigh less than 10 kg and, unlike the da Vinci system, can be attached directly to the operating table in order to optimize the workspace of each arm with respect to the others, much like the earlier Zeus system (Lafranco, 2004). The MiroSurge system consists of three 7 Degree of Freedom (DoF) MIRO arms: two manipulating laparoscopic tools and another manipulating an endoscopic camera (Institute of Robotics and Mechatronics, 2010). Force and torque sensors (mentioned previously) located near the tips of the tools provide feedback that is represented haptically with Force Dimension's Omega.7 haptic controllers. Three translational degrees of haptic feedback are possible with the Omega.7 controller. The ultimate goal in developing this technology is to be able to use the MiroSurge system to operate on a beating heart, thereby eliminating the need and risks of heart/lung machines.

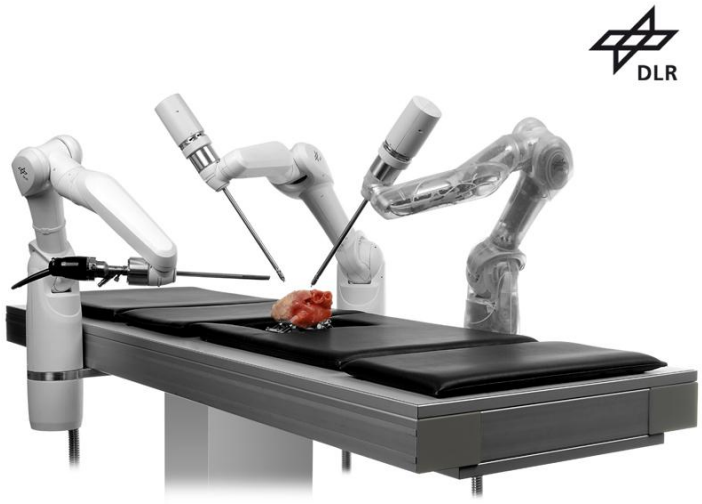

Figure 4: German Aerospace Center's MiroSurge System

Researchers at the Technical University of Eindhoven have developed the SOFIE (Surgeon's Operating Force feedback Interface Eindhoven) robotic arm (Figure 5) as a means of improving upon the da Vinci

system (van den Bedem, 2008). After performing field studies on robotic surgeries with the da Vinci, SOFIE was designed with the following design improvements in mind: connection to the operating table for easier set-up; additional DoFs at the instrument tip to improve organ approach; reduced system size; and reduced costs; and force feedback for reduced operating time and increased patient safety.

Figure 5: Technical University Eindhoven's SOFIE robot

The University of Hawaii-Manoa has built a simple, low cost, modular system for performing laparoscopic surgery (Figure 6) (Berkelman & Ma, 2009). This system has small, lightweight manipulators which can easily be clamped to the table, allowing them to be reconfigured with minimal hassle. These arms are designed such that the entire assembly may be placed in an autoclave, allowing for simple sterilization. This system does not include force feedback, but is manipulated with a controller which could provide haptic feedback. This arm eliminates the need for a remote center, by directly manipulating the arm tool from around the incision.

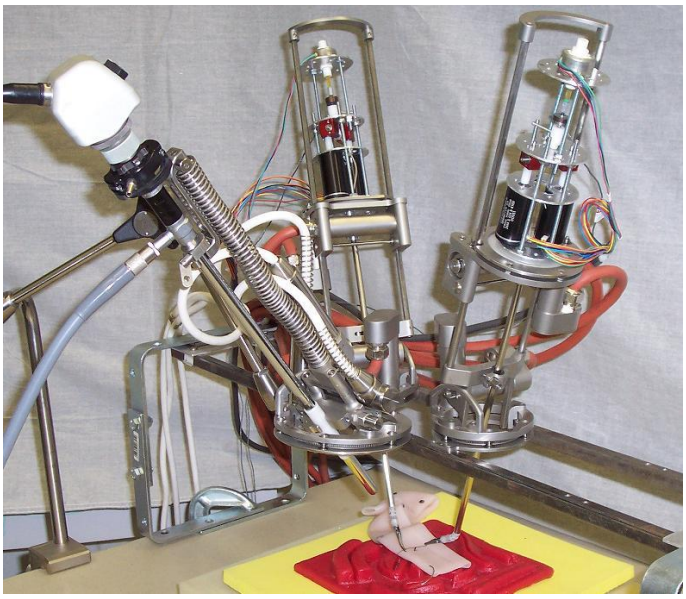

Figure 6: University of Hawaii-Manoa's Laparoscopic Surgery Robot

The BioRobotics Lab at the University of Washington is in the process of developing and testing the RAVEN telerobotic system (Figure 7) (Hannaford B. e., 2009), which is specifically aimed at researching the effects of long distances on telesurgery. In 2007, this system was successfully tested in the NASA Extreme Environment Mission Operations (NEEMO) 12 Mission. The system was operated in an underwater lab off the coast of Florida from stations in Ohio, Florida and Washington. Although the RAVEN is currently teleoperated with Sensable's PHANTOM Omni controllers, haptic feedback has not yet been implemented.

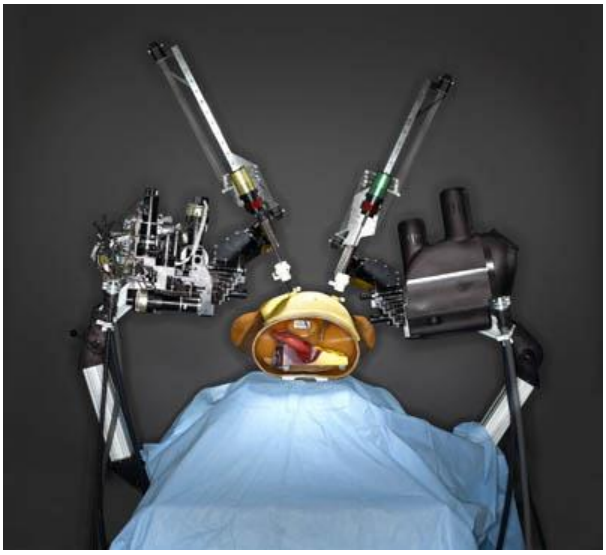

Figure 7: University of Washington's RAVEN Telesurgical System

Objectives

In order to more completely understand the state-of-the-art of modern telesurgery, a surgery performed with a da Vinci Si system was observed at the Boston Children's Hospital. From watching the surgery in its entirety several observations were made:

- The da Vinci system is very large and can be difficult to place next to the operating table.
- Depending on the arm configuration needed for the surgery, positioning the fourth arm for the extra tool can be unwieldy as it needs to wrap around the other arms from the central podium and can often interfere with the movements of the other, more critical arms.
- There is a need for more than two tool arms and a camera arm in some surgeries. In this specific case, a manual laparoscopic tool was used to hold the patient's liver away from the surgical area and as a means of passing needles and other supplies to the da Vinci tools.

These observations were verified by the hosting surgeons, who believed that a standalone arm that could be used in conjunction with the da Vinci system would be a commercially viable product to hospitals that have already invested a large amount of money into the da Vinci system. Although the commercialization of this project was decided to be outside of the scope, the possibility of commercialization drove several of the design requirements for the project at hand.

The immediate objective for this project was to create an arm and control system that could consequently be used to research the effects of haptics on telesurgery. With this goal and the subordinate goal of developing a commercially useful product, the following design statement was proposed:

Develop a surgical arm and controller that can manipulate da Vinci tools and be used alone or in conjunction with the da Vinci Surgical System. Additionally this system should be modular to allow the use of multiple arms, and be suitable for use in studying haptics and telesurgery.

The first half of the design statement describes the overarching requirement for the mechanical aspects of the system. The ability to manipulate da Vinci tools is especially fitting for both of the overall goals. Using available tools instead of creating them from scratch allows for attention to be paid primarily to the other systems in an effort to expedite the proposed research with the system. Furthermore, hospitals that have already invested in da Vinci tooling are more likely to adopt this system if it does not require further investment in tooling.

The software architecture and controls of the system are described by the second half of the design statement. Haptic feedback imposes a significant requirement on the communication protocols used by the system.

Mechanical Design

Requirements

Of the original list of design requirements the following applied directly to the mechanical aspects of the arm design and were kept in mind throughout the design process. These requirements were compiled using the design statement as a guide with inspiration coming from background research and discussions with interested parties.

StandAlone Surgical Haptic Arm (SASHA) should be able to manipulate a da Vinci Si tool about a remote center.

A remote center is necessary for any system performing laparoscopic surgery and can be maintained through either mechanical or software means. An early and major design decision was determining which approach would best suit the SASHA system. However, no matter the approach, a minimum of three DoFs is necessary to position the tool tip anywhere inside the abdomen.

SASHA should integrate the torque sensors developed by Andrew Marchese and Hubbard Hoyt for the original iteration of this project (Figure 8**)** (Marchese & Hoyt, 2010)

These unique torque sensors provide a means of directly measuring the torques applied to the da Vinci tool and therefore the forces being applied to the tool tip. Using these torque sensors is also a more direct method of measuring torques than by inferring the torque through ideal motor characteristics.

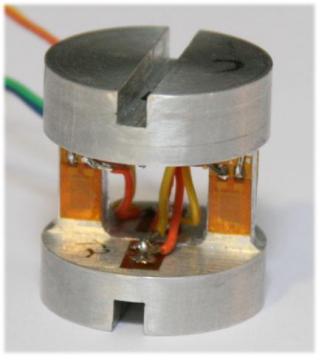

Figure 8: Strain Gauge Based Torque Sensors

SASHA should provide tool tip forces and speeds suitable for laparoscopic surgery.

The proper tool tip force was determined to be around 20 Newtons in any direction, which is more than 3 times the maximum force that inexperienced surgeons use to tie sutures (Kitagawa, Okamura, Bethea, Gott, & Baumgartner, 2002). The necessary tool tip speeds were determined by observing videos of da Vinci operations. Using approximate timing techniques and the distance traveled compared to the known length of the tool tip, it was determined that a tip speed of 3 cm per second would be more than suitable for this application.

SASHA should be able to work in a space large enough to facilitate laparoscopic surgery.

Through discussions with surgeons at Boston Children's Hospital, a suitable workspace of the tool tip inside the body was determined to be a 6-8 inch diameter sphere. A larger workspace is not necessary because of the limited space available in an average human abdomen.

SASHA should be easy to position before surgery or testing.

This means that the robot should be easily attached wheeled up to the operating table. Attention should also be paid to facilitating the fine positioning of the RCM.

Design Iterations

Initial Designs

Early design concepts were based loosely on SCARA type and serial robot arms. These types of arms are used heavily in industrial applications, where they can have flexible workspaces and fairly straightforward mechanics and kinematics. Two early concepts can be seen in Figure 9. The first concept uses a planar motion SCARA robot to manipulate a passive ball joint attached to a tool driver. An attachment grounded at the robot base would hold the tool shaft to maintain a remote center. The other concept shows a serial manipulator with a linear slide for inserting the tool, however the shown configuration does not maintain a constant remote center if all joints are active.

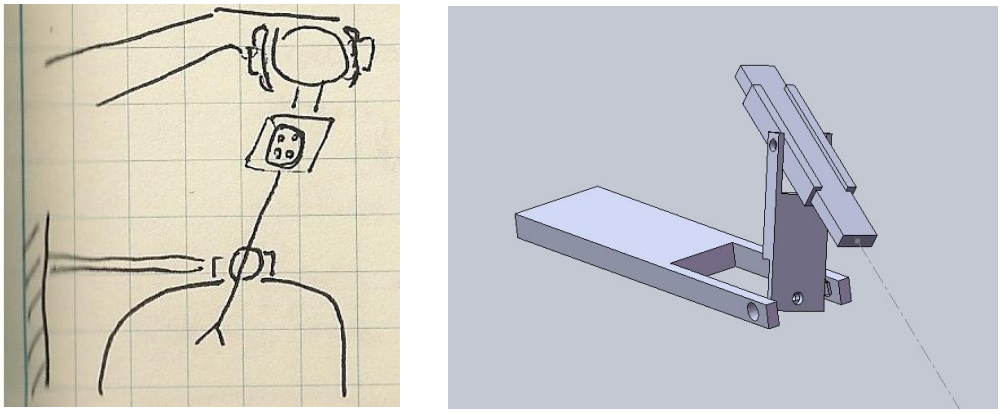

Figure 9: Early Design Concepts

It was decided to continue developing a serial arm because SCARA arms can be heavy and take up a lot of valuable space next to an operating table. Furthermore, a serial manipulator is much easier to prototype in the limited time available. For the second iteration (Figure 10) of the serial design concept, a further link was added to the system so that opposite links could be coupled in parallel to allow for the correct motions of the arm about a remote center. However, the issue of not maintaining a proper

remote center was not fixed until the next iteration. The solution to this issue was that the order of the joints needed to be reversed, as seen in the next prototype (Figure 11).

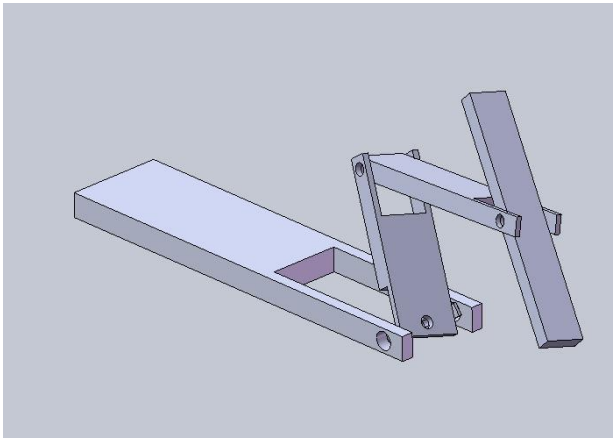

Figure 10: Second Design Iteration

The third iteration was the first to be physically prototyped (Figure 11). Physical prototyping was emphasized so as to manually investigate the motions of the design concepts and as a means of checking design decisions before committing too many resources to a design. Using laser cut acrylic and PVC piping as axles; it was possible to construct and manipulate the structure and investigate the size and workspace of the proposed arm. For this prototype, the size of the arm was based on the size of the plastic readily available and the workspace of the laser cutter.

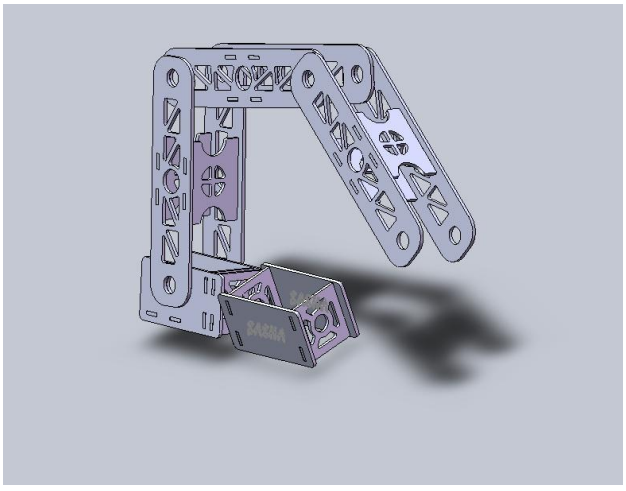

Figure 11: First Physical Iteration

Next, more investigation was put into the sizes of each of the links before constructing a full size prototype (Figure 12). The first approach to determining link lengths was looking into the average size of human adults, however applicable data was not immediately available and another analytical approach was used instead. Average operating room tables are approximately 19 inches wide, and it was decided

that the arm should not need to reach all the way across the table when standing straight up. Thus, the length of the upper horizontal link was decided to be around 17 inches. This length allows for the robot to be positioned on either side of the table and still reach almost the entire width of the table.

The length of the linear slide element was chosen based on the amount of travel necessary inside the abdomen and the length necessary for setting up the robot. The initial requirements call for a workspace inside the abdomen of at least 8 inches. This in addition to the setup travel needed to fully remove the tool from the trocar, which is the entry port into the abdomen, requires at least 15 inches of travel. As a slight factor of safety, a linear slide length of 17 inches was chosen. Consequently, the opposite link was modeled to be the same length.

A passive positioning system was also designed for this full scale prototype. A long arm free to rotate on both sides was placed between the operating table rail and the active base of the robot arm. This extra arm allows for the remote center to be configured in two degrees of rotational freedom along the lengthwise plane of the arm. An additional DoF is the arms placement along the table.

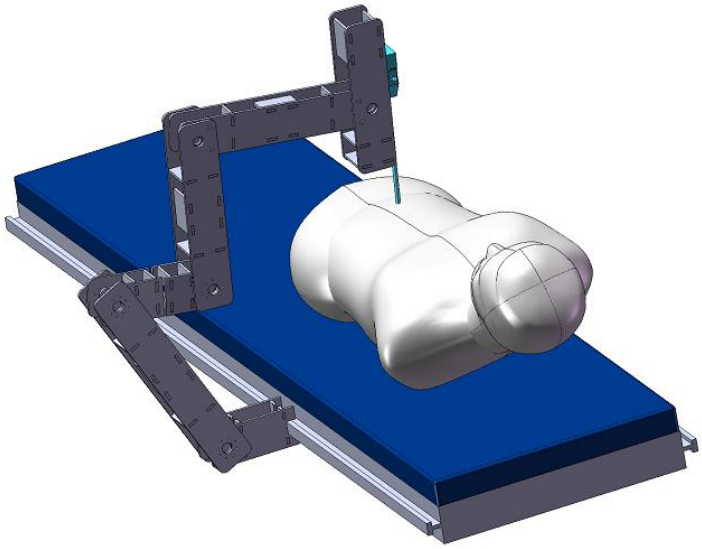

Figure 12: Full Scale Geometry Prototype

Final Design

The final SASHA design is a functional prototype using laser cut acrylic as the main structural material (Figure 13). The six main components of the arm were designed in the following order: the da Vinci tool interface that interfaces and controls the da Vinci tool; the tool carriage and linear slide that moves the tool tip in and out of the patient; the transmissions that control the rotations of the arm; the links that support the carriage and tool slide; and the passive positioning system that supports the arm and attaches to the operating table. Beyond the design requirements and overall objectives described previously, special emphasis was placed on manufacturability and the time required for machining each module. To this end, many identical parts are used in several modules. For instance, the acrylic plates

that define each component are held together by identical nut strips as this required only one repeated process instead of a series of different processes.

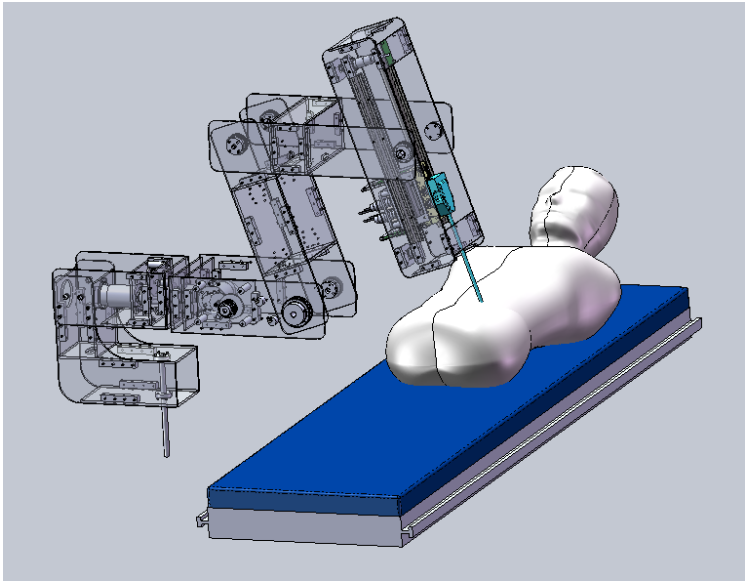

Figure 13: Final Mechanical Design

Tool interface

The first goal in creating SASHA was to be able to manipulate and sense tool tip forces. Consequently, the design of the tool interface would drive most aspects of the rest of the arm. As can be seen in the exploded CAD model in Figure 14, there are two main components to the tool interface: the da Vinci faceplate interface and the spring loaded motor module.

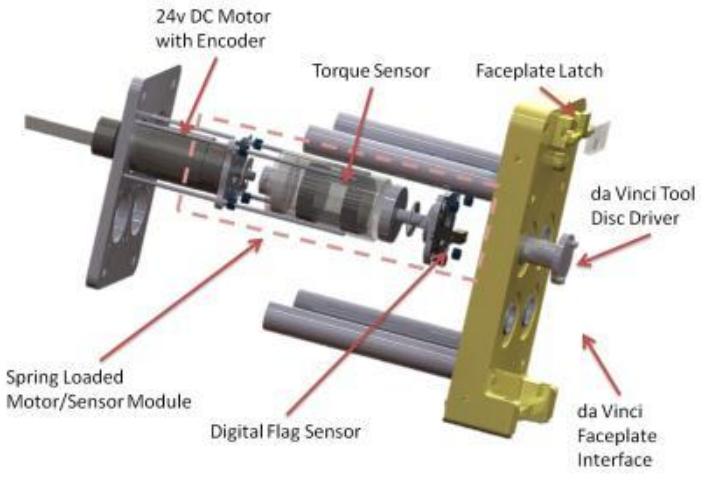

Figure 14: Exploded Tool Interface

The faceplate interface was designed to directly accept and hold a standard da Vinci Si faceplate so as to more easily replicate the interface and features of the da Vinci Si tool. To achieve this interface, a

faceplate was examined and found to have three distinct interface features: the lower tabs, upper locating hole, and upper latch area. The complements to these features were integrated into a single body that could be rapid prototyped using a 3D printer. This rapid-prototyped body was also designed to be the main structural element of the tool interface component.

Four discs in the back of the da Vinci tool are used to individually manipulate the four degrees of freedom of the tool tip. In the da Vinci Si system, these discs are driven by spring loaded interface bars that interface with the da Vinci faceplate discs which in turn interface with the discs of the tool. The sprung compliance of this system allows for holding the tool onto the faceplate and easily locking onto the discs.

In order to properly replicate this system, a similar spring system was required. The approach of this project differs from the approach of the previous attempt in that each of the driving discs of the tool interface are individually sprung, instead of all four discs being on the same plane and spring loaded in parallel. Although this extra compliance complicates the system, it also more closely replicates the functionality of the da Vinci system.

The drivers were designed to be directly connected to the low power motors that were used to drive them instead of using a cable system as in the da Vinci. Directly driving the interface discs greatly simplified the design over such alternatives as gearing or cable drive because of the complications inherent in spring loading such a mechanism.

As discussed earlier, the torque sensors developed and manufactured by the previous team were to be used in this design. The sensors were directly integrated between the motor and the tool driving disc.

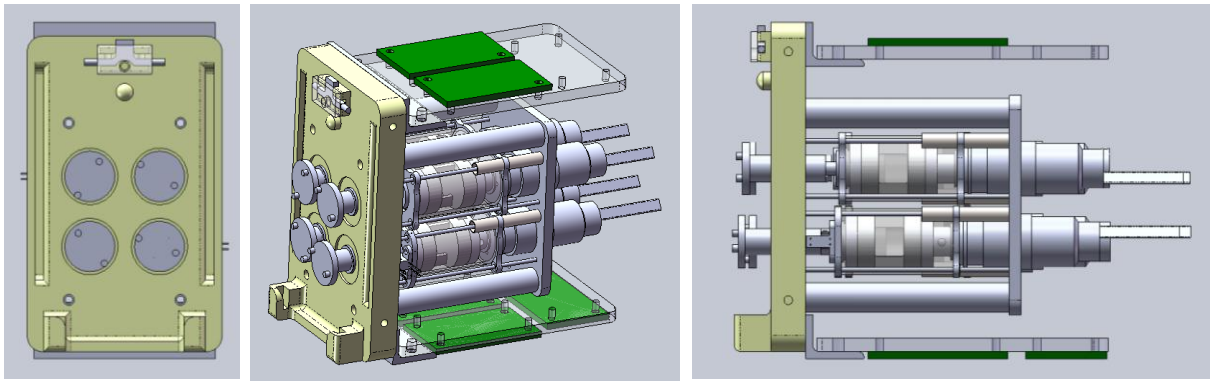

Figure 15: da Vinci Tool Interface

The exploded view above (Figure 14) shows how the sensor was integrated. On either side of the lexan tube that contains the torque sensor and its interface pieces, there is a lasercut plate that holds 4 plastic igus bushings, which ride on 2mm stainless steel guide rods between the interface plate and the back plate. On one end, there is a low power motor with an integrated quadrature encoder, and on the other end are a digital flag sensor, a plastic igus roller bearing, and an exposed axle for the interface driver disc

to interface with. The tube is glued to both end plates. Compression springs act against the back plate and the motor mount plate and shaft collars keep the springs from crushing the flag sensors. The interface driver disc passes through the interface body and is supported by a plastic igus bushing. Set screws are used to fix elements to shafts and pins are used to interface to the torque sensor and the da Vinci faceplate tool discs. One important note about the faceplate discs is that the pins are not on the same radius. Figure 15 shows the final CAD of the tool interface and Figure 16 shows the assembly of the first prototype complete with da Vinci faceplate and tool.

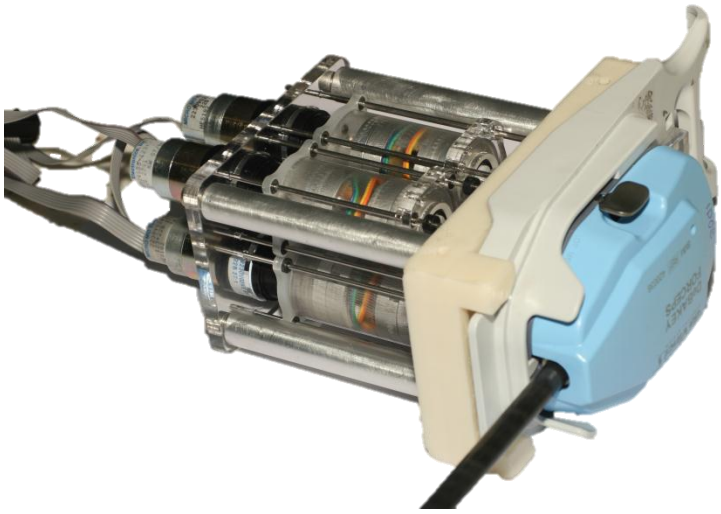

Figure 16: First Iteration Tool Interface

Carriage and linear slide

With the tool interface designed and the first prototype assembled, it was possible to design the linear slide. The driving design choice to this component was deciding how the tool interface would be supported and constrained to a linear path.

Commercial linear bearing rails, drawer rails and parallel shafts were all considered for the tool interface carriage to ride on. The availability and professional quality of commercial linear bearing rails and bearing components made available through the igus Young Engineer Support program made this option a clear choice. However, the accuracy of these rails also made it very important to maintain the rails in perfect parallel in order to avoid binding. The igus linear bearing components were very easy to integrate onto the sides of the tool interface with a simple laser cut acrylic plate to make the interface assembly into the tool carriage.

Both timing belts and lead screws were carefully considered for controlling the position of the carriage. Although a lead screw system can be highly accurate and provide inherent mechanical advantage, it would also add a significant amount of weight and bulk to the system. Additionally, it would have been very difficult to maintain the lead screw in parallel with the other guide rails. This is a problem that timing belts do not encounter because of their side-to-side compliance. The timing belt system also weighs significantly less than a lead screw system and takes up very little space in comparison.

The timing belt and igus linear rail system is very flexible in terms of lifting power and control. The system uses an open timing belt that can be tensioned using pressure plates on the plates that interface the tool interface to the linear bearing assemblies. The diameter of the timing pulleys were chosen so as to be able to lift the carriage and provide the required 20 N of extra force for surgery, however, as many as 4 motors can be used to move the carriage. The modules for powered and passive pulleys are the same and are therefore interchangeable. One or two motors can be used on either or both sides. This was an important feature because it was not known if driving motors on both linear rails would cause the carriage to twist slightly and bind. The interchangeability allows for testing of the system to determine which configuration produces the most desirable results. Figure 17 shows the system with one motor, and the photo in Figure 18 shows the assembled system with two motors on one side.

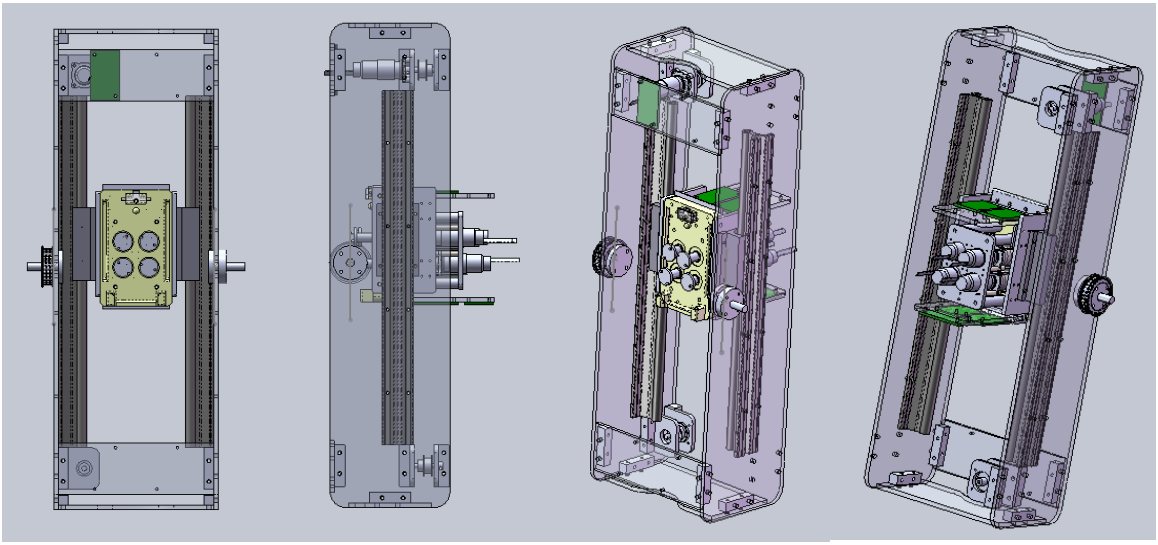

Figure 17: Tool Carriage and Linear Slide

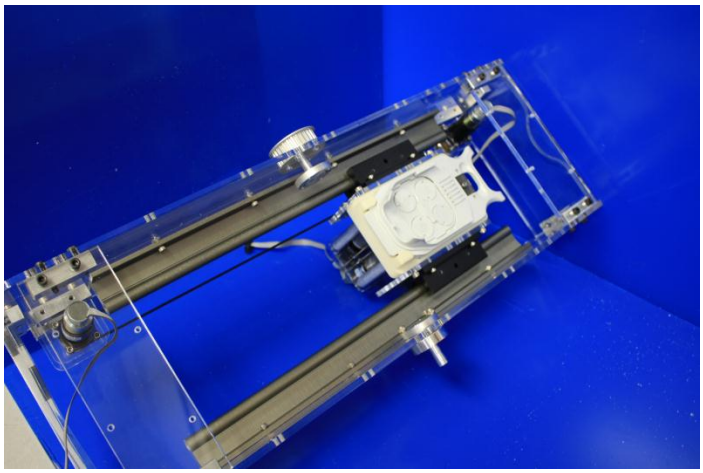

Figure 18: Assembled Tool Carriage and Linear Slide

Transmissions

The rotational degrees of freedom were designed to be run by high power motors that were donated by Comprehensive Power Inc. These motors were chosen out of the group of donated motors because they were already fitted with optical encoders and electromagnetic brakes. Both of these features were crucial to the project and would have been too expensive to purchase separately. Brakes are an essential feature of the transmissions as a safety feature if power is lost to the arm during operation. With a proper gear reduction, the brakes will be able to hold the arm without a power source.

The first transmission designed was the one that remains stationary while rotating the rest of the arm and can be seen in Figure 19. The necessary torque for this joint was determined based on the maximum location of the carriage during use and the 20 N force that could be applied to the tip. When the carriage is a maximum of 12 inches from the remote center, the 20 N force is therefore applied to a 6 inch lever arm, which results in a total of 7 ft-lbs on the working end of the transmission when the arm is perfectly horizontal. A safety factor of 2.5 was used since the rest of the arm was not included in the max torque calculations. The High power motor has a suggested running torque of 0.109 ft-lbs at 2950 rpm, which means that a reduction of 160.5 is necessary to move the arm when it is horizontal. Although this worst case is very unlikely, another small factor of safety was used and the final reduction used was 183.67 to 1. This results in a max torque of 20 ft-lbs at 16.14 rpm, which corresponds to a tool tip speed of 10 inches/sec at 6” beyond the remote center. These numbers are well within the design requirements. Additionally, the 1 ft-lb brake integrated with the motor will have more than enough braking force to statically hold the arm in its worst case configuration

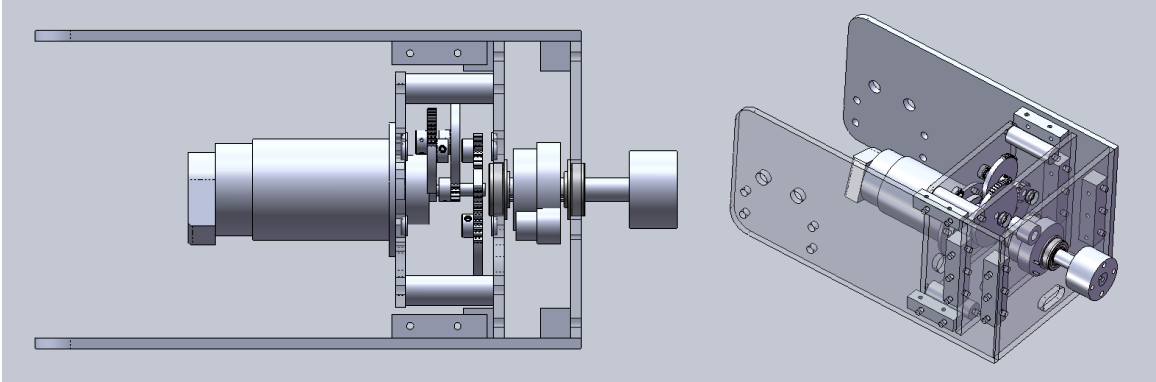

Figure 19: First Rotary Transmission

The next step was to choose the appropriate gears for the transmission. Originally, 32 pitch gears were chosen for each stage of the 4 stage transmission, but upon later inspection it was found that these gears would not be able to withstand the torque required of them. The equation used to determine the allowable tangential load on a gear is as follows:

$$W_t = \frac{S_W\, F\, Y}{P}\; x\; \frac{600}{600 + V}$$

W_t = safe pitch line load, lbs

S_W = safe stress, psi

F = gear face width, inches

Y = Lewis form factor

P = diametral pitch

V = pitch line velocity, feet per min.

All of the gears were chosen to be 303 stainless steel (with a safe stress of 30000 psi) and the Lewis form factor values were found in a table based on the number of teeth of a gear. The velocity values were based on the rotational velocity of the motor at the suggested torque through the applicable reduction. The Mathematica code used to calculate the safe torque on the gears is included in Appendix D: Safe working gear load calculations. This resulted in a mix of 32 pitch, 24 pitch and 20 pitch gears. By working close to the limits of the gears, however, the transmission was made as small and light as possible without using an expensive planetary or harmonic transmission. The final gear train is as follows:

$$motor_{torque} * \frac{60\ (32p)}{14\ (32p)} * \frac{60\ (32p)}{14\ (32p)} * \frac{60\ (24p)}{16\ (24p)} * \frac{40\ (20p)}{15\ (20p)} = \ 183.673$$

The second transmission designed is responsible for moving the parallel links of the robot (Figure 20). The transmission is separated by a timing belt reduction from the axle that it is ultimately powering. This extra space between the transmission and the link allows for the link to rotate about its axle without its

motion being overly limited by the physical location of the transmission. The required torque was estimated as the 5 lb carriage weight and a 20 N tool force on a 12 inch lever arm in addition to an estimated 2 lb weight of the links acting at 6 inches, which equals 10.5 ft-lbs. A safety factor of about 1.5 was used and the transmission was thus designed to hold around 15 ft-lbs.

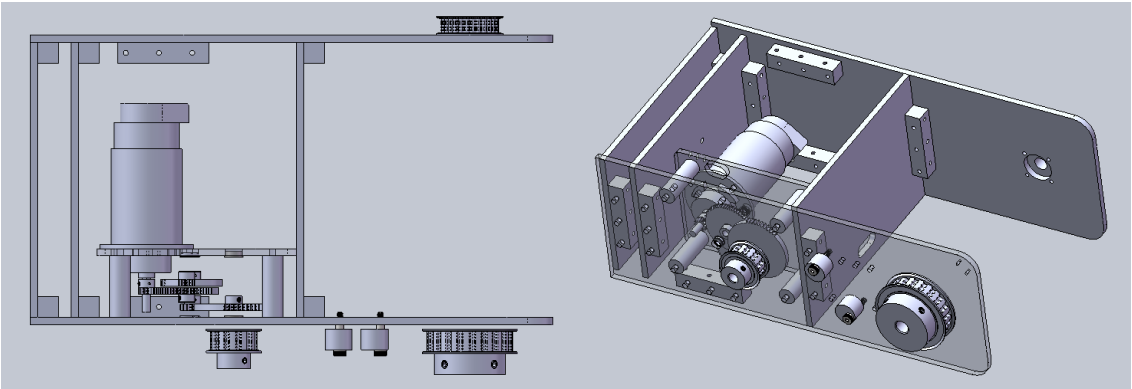

Figure 20: Second Transmission

The only difference in selecting the gears for this transmission was the timing belt reduction instead of the final gear reduction used in the previous transmission. The pitch chosen for these timing belts was L to ensure that the arm would not slip during use or storage. The final reduction was 134.69 to 1, which will move the tip greater than the minimum speed and will also allow the brake to hold the arm statically during storage or emergency shutdown. The gear train is as follows:

$$motor_{torque} * \frac{64\ (32p)}{14\ (32p)} * \frac{60\ (32p)}{14\ (32p)} * \frac{60\ (24p)}{16\ (24p)} * \frac{22\ (L)}{12\ (L)} = 134.69$$

The tensioning system used for tensioning the timing belts is a series of holes that allows for cantilevered shoulder bolts with either brass bushings or igus bushing material with eccentric holes. The eccentric holes allow for variable tension to be placed on the belt which can then be held constant by tightening a lock washer against the igus material. The variety of holes also allows for a wide variety of tensioning combinations.

Stainless steel was used for all load-bearing shafts. Set screws on flats were used for shafts smaller than ½" in diameter and undersized 1/8" keys were used on the ½ " shafts.

Links

The passive links were designed to allow for sufficient mobility without sacrificing the structural integrity of the robot (Figure 21). The construction style used was the same as that of the transmissions and linear slide section. Careful attention had to be paid to the widths of the links and the positioning of the timing belts. One pulley out of each pair was firmly attached to the link next to it, while the other side was fixed to its shaft via set screw on a flat. An equivalent tensioning technique to that of the second transmission was used to keep tension on the belts for the passive links.

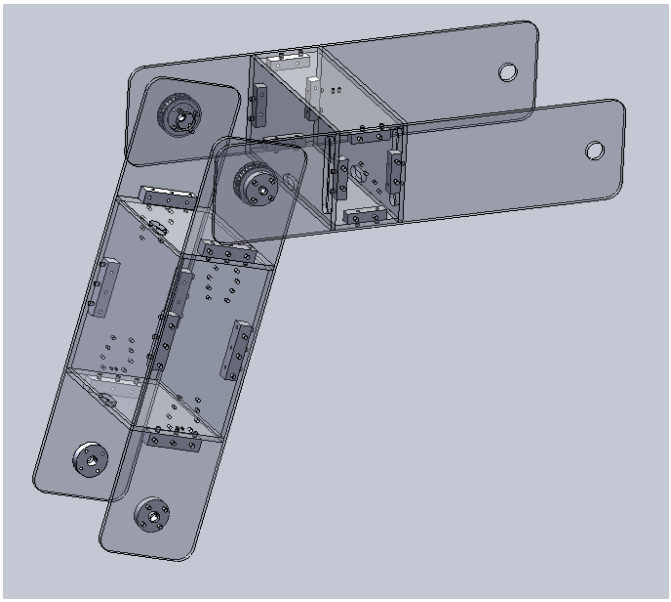

Figure 21: Passive Links

Passive positioning

The system used for passive positioning was greatly simplified from that of the previous prototype (Figure 22). A stationary 'L' bracket was used to support the arm on a single, ½" 303 stainless steel shaft. This shaft is held by the operating table rail clamp donated by Allen Medical Systems. This clamp allows for translation through the clamp, rotation of the axle, and rotation perpendicular to the length of the rail. With the addition of the translation along the length of the rail, this passive positioning system has 4 DoF, which is sufficient for testing purposes.

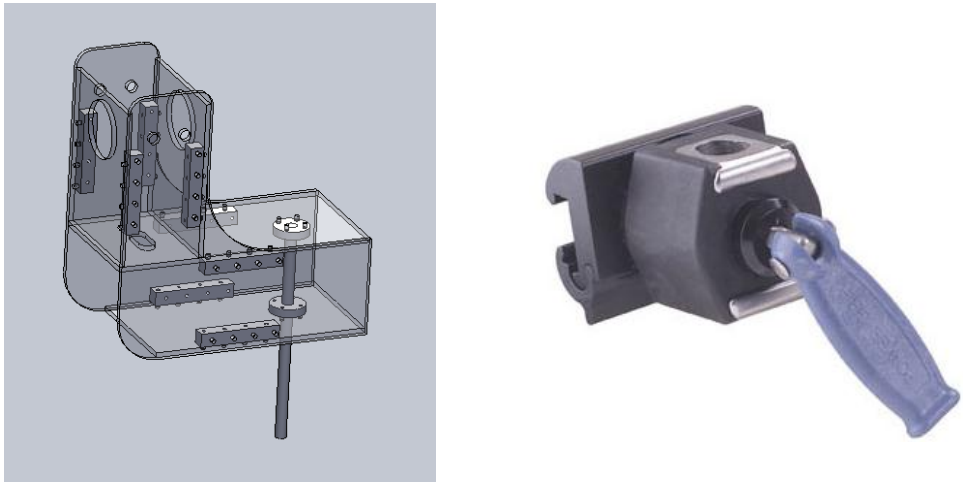

Figure 22: Passive Positioning System with Allen Madical Operating Table Clamp

Kinematics

The forward kinematics of the system are necessary for determining the location of the tool tip , which is crucial for calculating some of the forces on the tool tip based on the motor torques of the positioning motors. The kinematics of the tool location are decoupled from the orientation of the tool tip to make calculations easy. Figure 23 shows the dimensions of the robot that can be used for translational transformations of reference frames. The reference frame used in these calculations is centered at the point of the remote center with the z axis pointing directly down through the body and the x axis pointing along the length of the operating table.

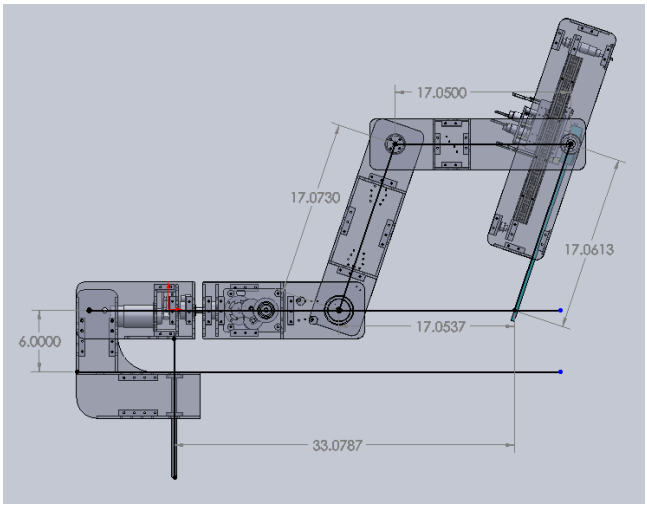

Figure 23: Linkage Dimensions

The definitions for the kinematic variables used can be seen in Figure 24 and Figure 25. The distance past the RCM is D, the angle between the tool tip and the YZ plane is theta, and the angle between the tool tip and the XY plane is theta. These variable correspond directly to the position of the linear slide, first transmission motor and second transmission motor respectively. The equations that govern the forward kinematics are the same that define the Cartesian coordinates of a sphere given polar inputs, and are as follows:

$$\begin{matrix} x \\ y = \\ z \end{matrix} \quad \begin{matrix} d\sin\theta \\ d\cos\theta\sin\varphi \\ -d\cos\theta\cos\varphi \end{matrix}$$

This leads to a Jacobian matrix as follows:

$$\begin{pmatrix} x' \\ y' \\ z' \\ \omega x' \\ \omega y' \\ \omega z' \end{pmatrix} = \begin{pmatrix} d\cos\theta & 0 & \sin\theta \\ -d\sin\theta\cos\phi & d\cos\theta\sin\phi & \cos\theta\sin\phi \\ d\sin\theta\cos\phi & d\cos\theta\sin\phi & -\cos\theta\cos\phi \\ 1 & 0 & 0 \\ 0 & 1 & 0 \\ 0 & 0 & 0 \end{pmatrix} * \begin{pmatrix} \theta' \\ \phi' \\ d' \end{pmatrix}$$

This Jacobian can be easily manipulated to find the torques on the motors from known forces at the tip.

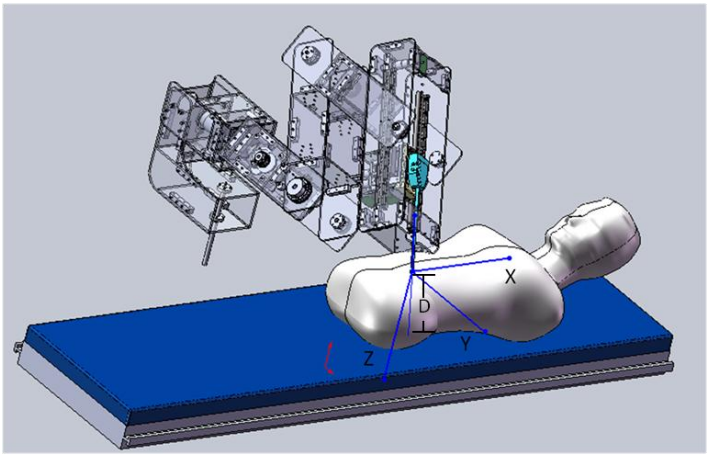

Figure 24: Body Coordinate System

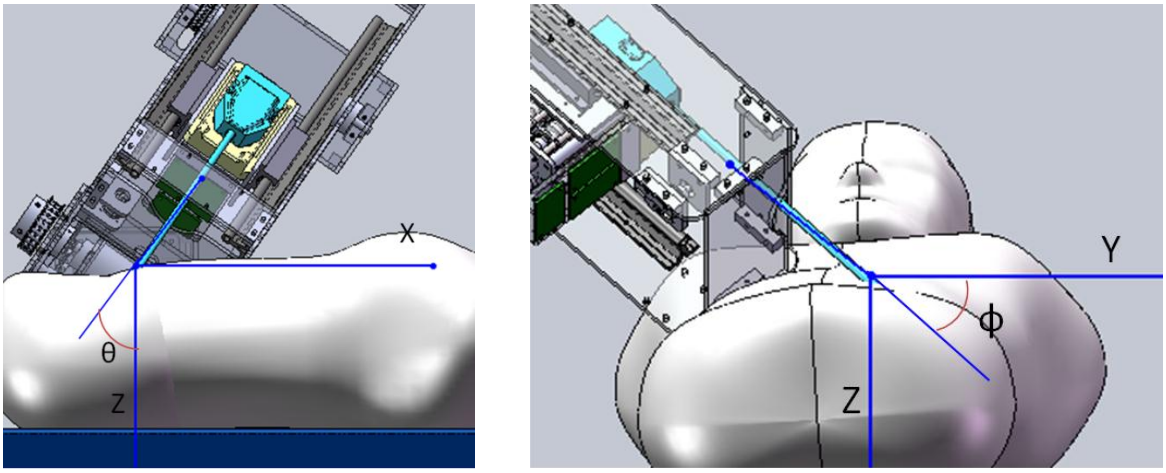

Figure 25: Arm Angle Definitions

Future Work and Improvements

Although this iteration has not been tested as a whole system, SASHA is nearly ready to be used as a first iteration research platform. However, the timing belts used to couple the opposing links are not capable of supporting the weight of the linear slide link. It is not possible to maintain the tension necessary to

keep the timing belts from slipping with the current tensioning method. The easiest and quickest fix to this challenge is replacing the timing belt system with a #25 chain and sprocket system. Chain is much easier to tension, especially with floating tensioners, and much harder to slip when properly tensioned. With this substitution and some thread lock in the set screws of the transmissions, it should be possible to start using SASHA as a research tool.

However, there are many areas that can be improved in a future iteration of the SASHA research platform. First, the torque sensors should be redesigned to allow for more elegant wire management, as the current system induces a significant amount of drag upon the sensor. The tool interface should also be redesigned to eradicate or minimize all sources of drag. The utility of the passive positioning system could also be improved, especially given a laser guidance system or a similar method of precisely positioning the remote center. Additionally, the entire system could be made significantly smaller and lighter with a different structural style which would significantly improve its utility and transportability. While the laser cut acrylic is appropriate for the first iteration and proof of concept, sturdier materials and structural techniques should be used to make the robot. The next iteration should be much more aesthetically pleasing.

Control System

Requirements

There were several requirements that were used to drive the design of the control system. The major driving requirements for this project were to be able to use it for research into telesurgery and haptics. For this reason, the system needed to be able to be operated remotely as well as provide feedback fast enough to be useful to the user, which was determined through research to be approximately 1kHz. The controls also needed to be able to manipulate the motors on the arm in a controlled fashion, as well as read and act on position and force information for each of the joints of the arm.

The remote operation requirement meant that there need to be a clean break between the arm controller and the user interface. It also meant that there needed to be an easy method of extending the communications over potentially very long distances or inserting delays between the user interface and the arm controller. The simplest solution to this is TCP/IP connection, allowing for two separate processes to be run locally or for processes on separate machines to communicate over an Ethernet connection.

Controlling the arm requires being able to drive each of the motors on the arm, which means that motor controllers are necessary. These motor controllers also needed to be able to read the encoders on the motors to control the position and speed of the motor. Additionally, the output of the strain gauges used for force sensing needed to be measured and reported back to the user.

Modularity was an additional factor taken into consideration, as this would help to minimize design time. This would also mean that debugging would only need to be performed once and any damaged

boards would be cheaper and easier to replace. Simple wiring was also desirable, as wires can be very difficult to route on a moving piece of hardware.

Design Overview

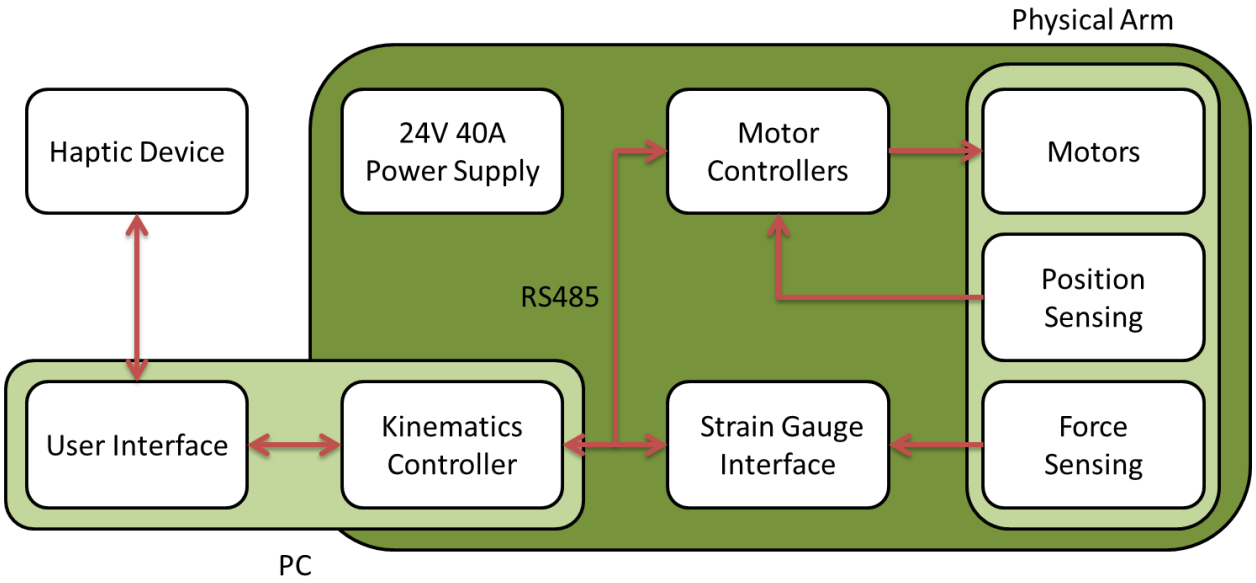

Figure 26: Control System Block Diagram

Based on the design requirements, a top level design for the control system was developed, as seen in Figure 26. A kinematics controller program, running on a PC or embedded Linux system, acts as the master controller for the arm. Each motor has its own motor controller which can read the attached encoders. This allows for fast control loops to be run onboard without the delay of communications. A separate strain gauge interface board reads, amplifies and converts the strain gauge reading to a digital signal. Each of the motor controllers and the strain gauge interface communicate with the host controller through the same RS485 connection. A USB to RS485 converter capable of speeds up to 3MBaud allows for the kinematics controller to communicate with these boards. A TCP/IP connection allows for the kinematics controller to communicate with the user interface, which can be running on the same or a different computer.

The motors used on this project were six small Low power brushed DC motors and 2 larger High power brushed DC motors. The Low power motors, part number 2230V024S, include integrated magnetic encoders and a 27:1 gear reduction. These are 24 volt motors with a free speed of 9000 RPM, stall torque of 12 mNm, and stall current of .5 amps. The nominal power rating is 2.82 watts. The High power motors, part number 14203D475, include an integrated 256 CPR optical encoder. These are 24 volt motors with a free speed of 3390 RPM, stall torque of 1.1225 Nm, and a stall current of 17.4 amps. The nominal power rating is 46 watts. The High power motors also have an attached brake which is released by applying 24 volts across the leads. In addition to the encoders, each of the motors on the tool interface board have a beam break limit switch to allow for a zero position to be consistently determined.

Four of the small motors are used to manipulate the tool, and an additional 2 are used on the linear slide. Six low power motor controller boards were necessary to control these. Two of the large motors

with brakes were used to control the gross positioning of the arm, so two of the high power motor controllers were necessary. Only one strain gauge interface board was needed to interface to all four of the strain gauges.

There were several reasons for doing multiple motor controllers. By doing one motor controller per motor, motor controllers could be designed for each distinct type of motor, and then manufactured multiple times, minimizing design time. This also meant that if one of the motor controllers broke, it would be substantially cheaper to replace do to identical parts and simpler atomic components. This also allows for optimal placement of the motor controllers in relation to the motors, minimizing the length of the motor and encoder leads. Since each motor also has its own digital signal controller, control loops can be run quickly and without having to share resources to control multiple motors. This also makes it trivial to add motors or reconfigure the arrangement. This also means that the boards could also be used as motor controllers in other research projects.

Each of these controllers and the sensor interface board also needed to be able to communicate with the kinematics controller. RS485 was selected for this task for several reasons. Because of the potentially noisy environment, a communications standard with a differential signal was desirable. To minimize the amount of necessary wiring, a standard that would allow for either daisy chaining or a multi-drop standard was necessary. This standard also needed to be capable of data rates greater than 1Mbaud to ensure that control information and feedback could be streamed to and from each of the controllers at greater than 1kHz, the cutoff for useful haptics. The maximum speeds for CAN were right around this 1Mbaud limit, and the CAN adapters for PCs were expensive. I^2C was similar to CAN in these respects. SPI was fast but lacked a differential signal. RS232 also lacked a differential signal. RS485 and Ethernet both met the requirements, with RS485 requiring an inexpensive USB adapter and Ethernet working natively on modern computers. Ethernet, however, required substantially more expensive components on each of the boards and also had a substantially higher software overhead than RS485. Also, while most micro controllers have a UART, there are fewer that have Ethernet interfaces, and those are generally more expensive. For these reasons, RS485 was selected as the method to communicate with the motor control boards and the strain gauge interface.

Each of the motor controllers and the strain gauge interface also required a microcontroller to handle the communications and any motor control and sensor input. It was decided that all of these should be the same controller to minimize the amount of additional design and research that would be required to use multiple different microcontrollers. The chosen microcontroller needed to require as few external components as possible. This meant that the microcontroller needed to natively handle the chosen communications protocol, have an ADC, quadrature encoder decoder, and hardware PWM generation. Several lines of Microchips PICs, and Texas Instruments Stellaris and Piccolo series microcontrollers were considered. These were all similarly priced and had similar features, with the Stellaris line having the advantage of an Ethernet interface. Since it was decided to go with RS485, however, the deciding factor came down to familiarity, and the TMS320F28031 from TI's Piccolo line was selected. Familiarity was considered to be an important factor since it reduces the amount of time spent learning the development tools and reduces mistakes. Texas Instruments was also known to have excellent documentation and sample for their products.

It was also decided that minimizing the wiring and external components needed to run each of these boards was a priority. To accomplish this, each of these boards has an on board switching regulator to provide the 5V logic supply, and an additional linear regulator off of the 5V to supply 3.3 volts to the digital signal controller. This allows for each of the board to be run off of only 4 wires, 2 for RS485, one 24V power and one ground connection. Requiring a low voltage control supply off board would have required that additional wires be run to each board. Since the arm is moving it is best to simplify the wire paths.

Common Circuits

In order to reduce design time several circuits were repeated on each of the three board types developed as part of this project.

Digital Signal Controller (DSC)

The same digital signal controller, the TMS320F28031, from Texas Instruments was used on each board. This controller has 16 ADC inputs, 12 PWM channels, a UART, and a quadrature encoder interface. This controller also runs at 60MHz, has 16kB of ram and 64kB of Flash, and requires a single 3.3 volt supply. This makes it suitable for use on all three of the board designs. A JTAG port was also broken out on each of the boards, allowing for them to be debugged and programmed easily.

Each of the boards also has a header block which carries out 2 analog inputs, 2 general purpose IO pins, and 5V and ground, allowing for additional sensors to be included later.

5 Volt and 3.3V Supplies

In order to minimize the wiring to each of the boards it was decided that each should work with only a single 24V supply. The DSC's however required a 3.3V supply and the encoders and the H-bridge require a 5V supply. This meant that on board voltage regulators were required.

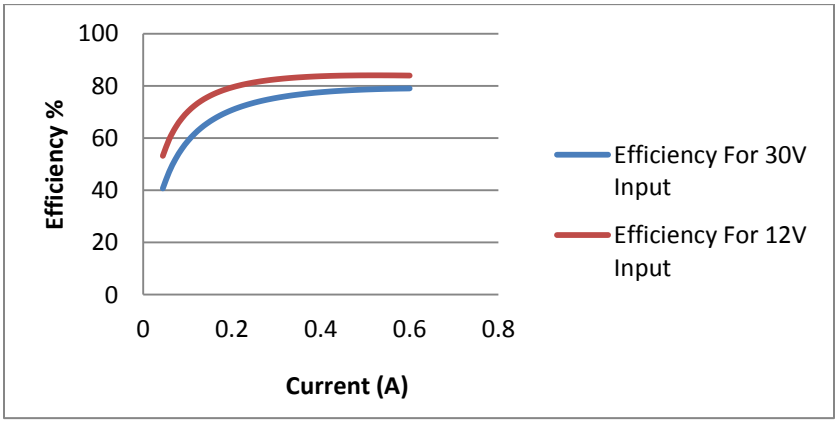

Figure 27: SwitcherPro Calculated Buck Converter Efficiencies

To provide the 5V supply it was decided to use a switching regulator since a linear regulator would be very inefficient at reducing the voltage by that amount. A buck regulator was designed using TI's SwitcherPro design tools to be able to provide 600 mA at 5V. The predicted efficiency can be seen in Figure 27, which can be compared to an expected efficiency of a linear regulator of 40% for 12V in and

16% for 30V in. The characteristics, including voltage ripple calculated by SwitcherPro may be seen in Table 1. This meets the current requirements for each of the boards, so the same switching regulator could be used on all of them. A TPS5410 was used as seen in Figure 28 to construct the buck converter.

Table 1: SwitcherPro Buck Converter Characteristics

Parameter	Minimum	Maximum	Nominal	Maximum	Units
Input Voltage	12	30	-	-	Volts
Input Ripple	-	-	-	170.9	mVp-p
Output Voltage	-	-	5	-	Volts
Switching Frequency	-	-	500	-	KHz
Estimated PCB Area	-	-	176	-	mmÂ²
Max Component Height	-	-	-	8	mm

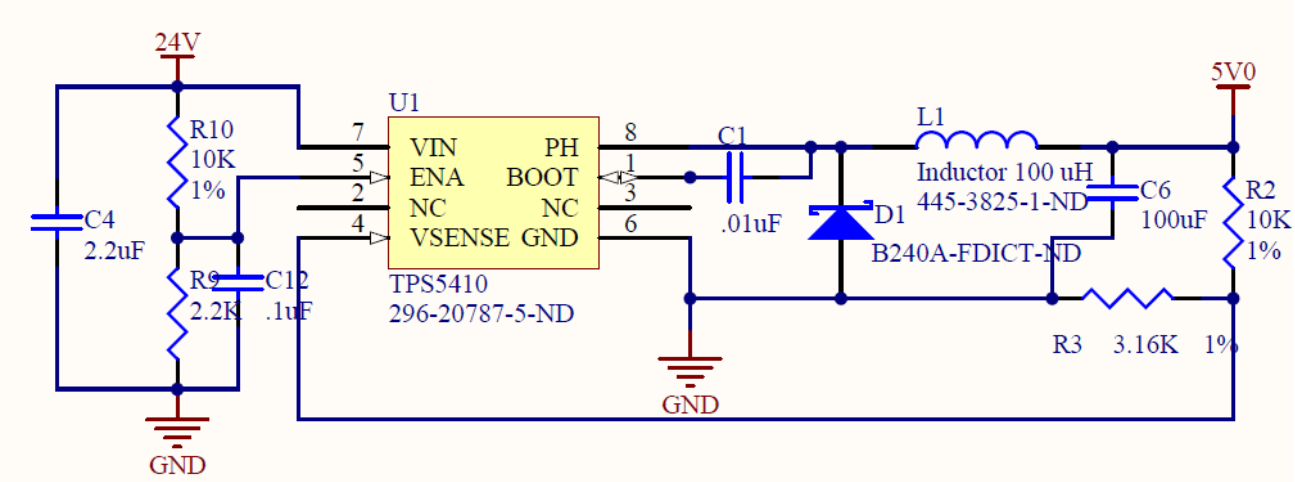

Figure 28: 24V to 5V Buck Converter

A 3.3V supply was also required for the DSC and analog components. A linear regulator was used to step down the 5V supply to 3.3V. Since the voltage difference was small, this could be done efficiently. A REG113 with a current capability of 400mA was used for this purpose. This had a substantially lower part count and cost than the switching regulator.

RS485 Interface

In order to communicate with the kinematics controller, each of the boards required an RS485 transceiver to do the level shifting between RS485 and the UART on the DSC. An SN65HVD11 was used for this purpose.

Low Power Motor Controller

Requirements

The low power motor controller needed to be able to drive a single 24V motor with a stall current of .5 amps. It additionally needed to be able to read the encoders and beam break limit switches. Measuring current was also desirable to serve as a redundant means of determining the forces at the tool tip.

Component Selection

To drive the motor, an H-bridge circuit was needed. An integrated solution was found in the L293D. This is capable of driving at up to .6 amps and will accept 3.3 Volt logic signals to drive it. This allows for PWM signals to be used to drive the motor in both in forward and reverse at varying speeds.

The encoder in the motor has a 10kOhm pull up resistor to 5V, which is pulled down by a transistor. By placing a 20kOhm pull down resistor on the output line, this limits the voltage to 3.3 Volts which is suitable for the DSC.

In order to sense the current into the motor and into the board a shunt resistor and shunt current monitor was used. The INA170 is a bi-directional current sense monitor. This amplifies the voltage across a low value resistor which is then read by the DSC. This circuit may be seen in Figure 29.

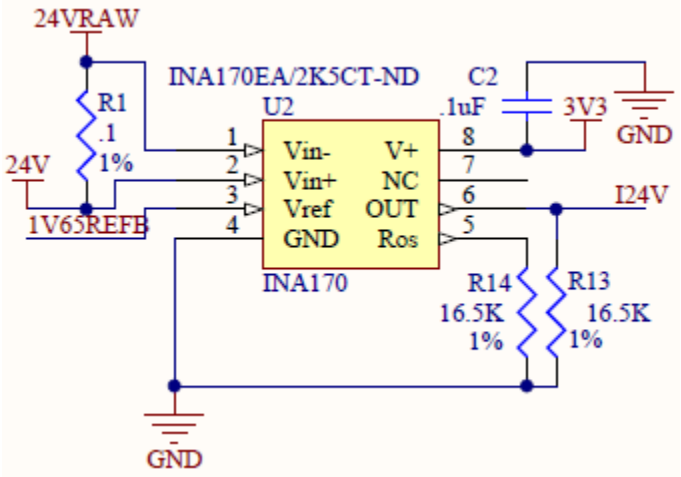

Figure 29: Current Shunt Monitor

Current Status

The low power motor control boards were the first to be designed, assembled, and programmed and they are the most complete in terms of testing and programming as a result. One of the completed boards may be seen in Figure 30. The complete design including a bill of materials, schematic, and layout may be found in Appendix A: Low Power Motor Controller. The motors have been driven with these under loads from none to stall condition. RS485 has also been tested and works, with commands being able to be received and sent. The encoders also read properly, and the beam break limit switches are able to properly zero the encoder count.

The software for these boards currently allows for PID control of position. The communications software correctly filters out commands based on device address and allows for the kinematics controller to send position commands to the board, and the positions are reported back to the kinematics controller correctly.

The 24V in current sensor seems to work properly, but unfortunately the INA170 is only a high side current shunt monitor, so the current sensing into the motor does not work. This can be inferred, however, from the motor characteristics, speed and duty cycle or from the duty cycle and 24V current sensor. Fortunately this is non-critical because the strain gauges are the primary method of measuring forces in the tool tip.

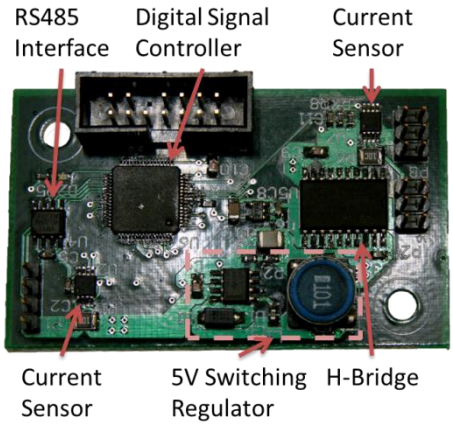

Figure 30: Low Power Motor Controller

Future Work and Improvements

There is a significant amount of room for software development on these boards, since only one control mode is currently supported, and most of the desired information is not currently calculated. Currently, only position control mode is supported, other control modes would be velocity control mode and current control mode. Future software development should add more control modes and fault detection. The ADC is also currently only partially configured and only reads from 2 inputs. Software should also be written to allow for constants such as zero positions, PID gains, and ID number to be stored and modified in the Flash memory.

A different method for current sensing should also be used. One suitable method would be to use hall-effect current sensing similar to what is done on the high power board. This would eliminate the current problem of having to deal with measuring a small difference in voltage that swings from one rail to the other.

In wiring these boards, it was also noted that they were difficult to daisy chain as only one set of wires would fit into each board. This meant that cables had to be spliced together before they entered the connector for each board. A better solution would be to use 2 sets of connectors on each board so that each board would be connected to the previous one. A different style of connector would also be helpful, since the headers that were used do not lock in place. A suitable replacement may be the Micro-

Fit 3.0 line from Molex. The connectors are also currently unlabeled, so either silk screened labels to specify polarity or keyed connectors such as the suggested Molex connectors would reduce the likelihood of wiring the board in reverse.

High power Motor Controller

Requirements

The high power motor controllers needed to be able to control 24V motors with a stall current of approximately 20 amps. It also needed to be able to release the brake on the motors and read the encoders on the motors. These also needed to be able to measure the current in the motors as this is the only way that we currently have to measure the forces in the gross positioning of the arm.

Component Selection

The first component to be designed on the high power motor controller was the motor control bridge and the gate driver. Since this needed to be able to drive 20 amps, it was determined that discrete MOSFETs would be more readily available than any sort of integrated H-bridge. The IRFR1205 N-channel MOSFETs were used because of the surface mount package, 44A capacity, and 55V standoff voltage. This provided for a substantial safety factor on current, which was important because the only heat-sink was the power planes that the MOSFETs were attached to. 3 half H-bridges were formed from this, 2 for the motor control and one for releasing the brake.

All N-channel MOSFETs were used because of their higher current capacities, but this necessitated the use of a gate driver. The gate driver selected was the A4935 from Allegro. This allows for driving both high and low side of all three half bridges, is compatible with 3.3V logic, and included an integrated supply for driving the gates. The three half bridges and gate drive circuitry may be seen in Figure 31.

Due to the issues with the current shunt monitor used in the low power boards, hall-effect current sensors were used on this board. The ACS709 from Allegro was used. This allows for 37.5 Amps to be measured in either direction without regard to the potential at those points.

The encoders drive the signal to 5V or 0V. To interface these to the DSC a simple resistor voltage divider was used to step the voltage from 5V to 3V.

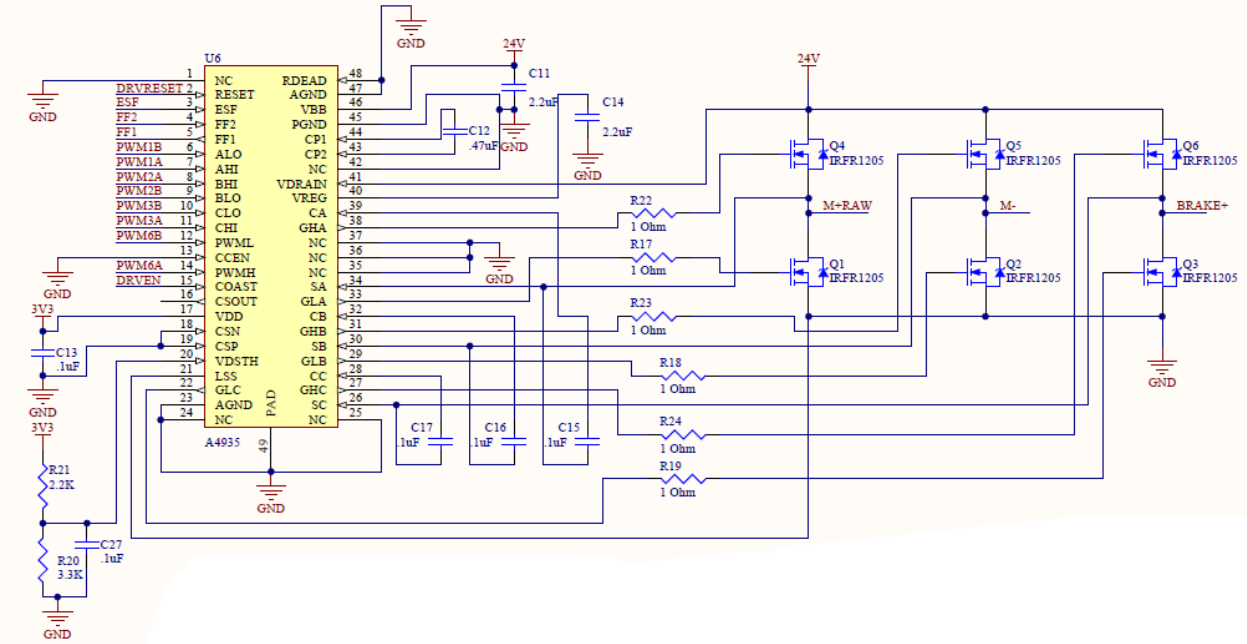

Figure 31: Gate Driver and 3 MOSFET Half Bridges

Current Status

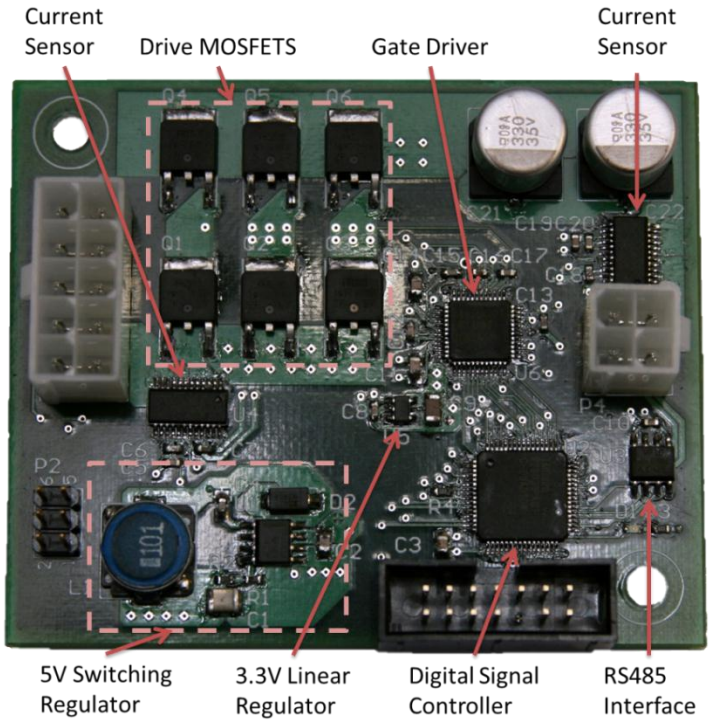

Figure 32: High power Motor Controller

It has been verified that code can be loaded onto the DSC. The drive circuitry has also been tested and is able to drive a motor in both directions as well as release the brake. Most of the drive code from the

small motor controllers should work with minimal modifications on this board, but this has not been tested yet. The current sensors and the encoders also need to be tested. The bill of materials, schematics, and PCB layout may all be found in Appendix B: High power Motor Controller. The completed board may be seen in Figure 32.

Future Work and Improvements

The software developed for the low power board should work with very little modification on the high power boards. The gate driver provides fault detection and these faults should be acted upon and reported back to the Kinematics Controller. The code also needs to be sure to output complementary PWMs for the high and low sides of the half-bridges, as well as output a signal to disengage the brake.

One of the vias providing the 24V connection to the 5V regulator was missing because it was deleted by Altium. The cross hatch for this via may still be seen on the board though. Several of the vias connected to ground under C21 and C22 were also left unconnected by Altium. These should not greatly affect functionality, but both of these should be fixed on future iterations of the board.

This board could also benefit from doubling the incoming 24V, ground, and RS485 connections as described for the low power motor controllers. The current sensors and encoders also need to be tested.

Strain Gauge Interface

Requirements

The strain gauge interface needed to be able to take the voltage differences from the four Wheatstone bridges, amplify them, and read them into the DSC so that they could be reported back to the kinematics controller. The strain gauge interface also needed to be able to communicate with the ID chips in the tools.

Component Selection

For the instrumentation amplifier, the previous MQP used an AD620 with a gain of 1000 (Marchese & Hoyt, 2010). Since this was proven to work, the same instrumentation amplifier circuit was used, but re-scaled for 3.3 volts by adjusting the bias voltage to 1.65 volts, and a surface mount variant was used. Their results show that a .6Nm torque corresponds to a difference in voltage of approximately .9 volts. This circuit may be seen in Figure 33.

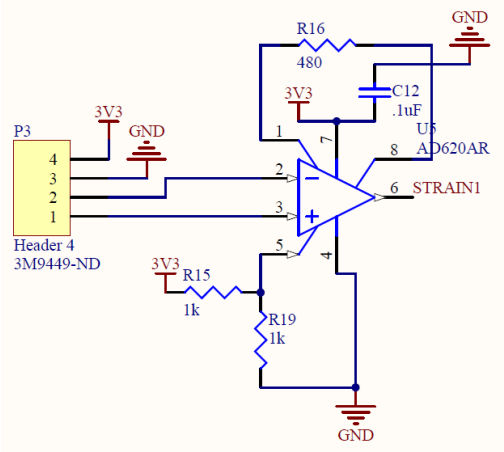

Figure 33: Instrumentation Amplifier

The da Vinci tools include a DS2505, a write-once device which contains tool and use information. This communicates over a 1-Wire interface, so a 1-Wire transceiver was included to allow for the DSC to communicate with the tool. The DSC has to bit-bang this serial port since it has one hardware UART that is being used for RS485. The 1-Wire transceiver used was the DS2480 from Maxim, and the circuit may be seen in Figure 34. An additional linear regulator, part number TPS79801, was also added to provide the 12 volt supply needed to write to the tool.

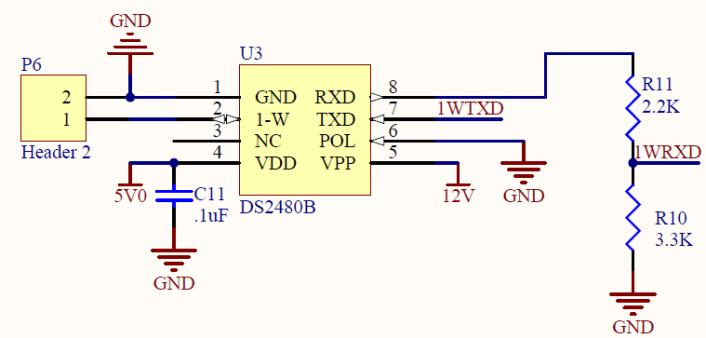

Figure 34: 1-Wire Interface

Current Status

The strain gauge interface has been assembled, but beyond confirming that the DSC can be programmed, nothing has been tested. The instrumentation amplifiers and the 1-Wire interface both need to be tested. The assembled board can be seen in Figure 35 and the complete documentation including the bill of materials, schematics, and PCB layout can be found in Appendix C: Strain Gauge Interface.

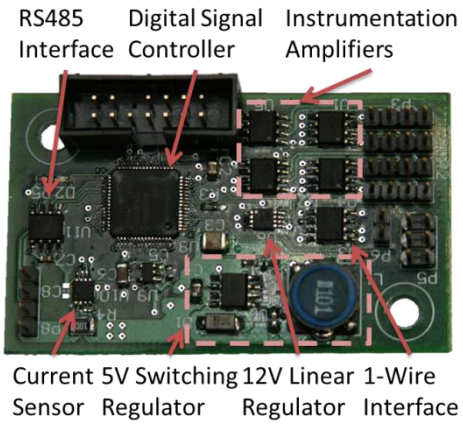

Figure 35: Strain Gauge Interface

Future Work and Improvements

This board would benefit from the same doubling of input connectors and switching to locking connectors that was described for the low power motor controller. This board had the additional problem of the JTAG connector interfering with one of the mounting screws.

The software for this board should be similar to the motor controllers, but it also needs to be able to talk with the da Vinci tools. This will require bit-banging the signal on two GPIO lines because there was only one UART. The instrumentation amplifiers also need to be tested. In fact, the gain of the amplifiers may need to be adjusted because the calculations that the gain was based on were based on oversimplified assumptions. The original assumption was that active portion of the torque sensor could be modeled as a cantilevered beam with only one captured end. This has led to an inaccurate model that can be fixed by modeling the torque sensor as two beams with both ends captured.

Kinematics Controller

Requirements

The kinematics controller needs to be able to communicate with the motor control and strain gauge boards, as well as be able to communicate with the user interface. The user interface connection is over TCP/IP, and is easily expanded over an Ethernet or Wi-Fi connection. The connection to the boards is accomplished by a USB-COM485-PLUS1 USB to RS485 adapter. This appears as a standard COM port to the host operating system.

In order to facilitate the use of this project in future research, a well-defined API for communicating with the boards is needed. This API needs to also make it clear how to add additional features.

Current Status

The Kinematics controller was written in Java and uses the RXTX library to interface to the RS485 adapter. The kinematics controller currently allows for writing and reading position values to each of the boards via the command line, addressing them by serial number. An API is being developed that will

have objects representing each of the boards that will allow for values to be transparently written to and read from them.

Communication Protocol

The kinematics controller acts as a master on the RS485 network, sending requests to the other boards which then send back a response. The requests from the kinematics controller are structured as seen in Table 2. This allows for the Kinematics controller to address a specific device, set what aspects of it are enabled, and set the control mode or other values through the command number and the command value.

Table 2: Request Message

Byte #	Contents	Description
1	's'	Start character
2	's'	Start character
3	Message Number	Echoed back to identify what message was sent
4	Device Address	Address of the device being talked to
5	Command Number	What to do with the data in the command value
6	Enable	Enable switching, brake, or other aspects
7	Command Value High	Value associated with the command
8	Command Value Low	Value associated with the command
9	Checksum High	Checksum of bytes 3-8
10	Checksum Low	Checksum of bytes 3-8

All of the boards listen to all requests, but they will only act on requests that are addressed to 0 or to their address number. When their address matches they will respond with the message structure seen in Table 3 for the motor controllers and in Table 4 for the strain gauge interface. This structure guarantees that the information critical for determining what forces should be reported to the user are sent back with every response. It also allows for other value to be sent through the command value. This also allows for fault reporting for the motor controllers, which may include things such as a low or high DC bus, or issues with the H-bridge or H-bridge driver.

Table 3: Response Message from Motor Controllers

Byte #	Contents	Description
1	'r'	Start character
2	'r'	Start character
3	Message Number	Echoed message number
4	Device Address	Address of responding device
5	Faults High	Each bit represents a fault condition
6	Faults Low	Each bit represents a fault condition
7	Position High	Rotational position of motor
8	Position Low	Rotational position of motor
9	Velocity High	Rotational velocity of motor
10	Velocity Low	Rotational velocity of motor
11	Current High	Current draw of motor
12	Current Low	Current draw of motor
13	Command Response High	Response associated with received command
14	Command Response Low	Response associated with received command
15	Checksum High	Checksum of bytes 3-14
16	Checksum Low	Checksum of bytes 3-14

Table 4: Response Message from Strain Gauge Interface

Byte #	Contents	Description
1	'r'	Start character
2	'r'	Start character
3	Message Number	Echoed message number
4	Device Address	Address of responding device
5	Strain 1 High	Strain Reading
6	Strain 1 Low	Strain Reading
7	Strain 2 High	Strain Reading
8	Strain 2 Low	Strain Reading
9	Strain 3 High	Strain Reading
10	Strain 3 Low	Strain Reading
11	Strain 4 High	Strain Reading
12	Strain 4 Low	Strain Reading
13	Command Response High	Response associated with received command
14	Command Response Low	Response associated with received command
15	Checksum High	Checksum of bytes 3-14
16	Checksum Low	Checksum of bytes 3-14

The checksums for both sending and receiving make it so that it is harder for corrupted messages to get through. The start characters make it easy for each board to synch to the start of a new message, and whether the message is coming from another board or from the kinematics controller.

Future Work and Improvements

The kinematics controller is far from complete. It currently only allows for position control communications with the low power motor controller. It will need to be able to support current and velocity control as well as handle faults and force feedback information from all of the boards. The API for communicating with each of the boards needs to be clearly defined as well.

The kinematics controller also needs to be able to perform the kinematics calculations for the positioning and forces at the tool tip, as well as be interfaced to a user interface. The user interface should visually represent the forces and allow for the user to control the arm using sliders. The user interface should also make use of the PHANTOM Desktop from Sensable to allow the user to manipulate the arm and receive three degrees of force feedback.

Discussion

There were several major accomplishments in this MQP:

- A da Vinci Si tool interface complete with torque sensors was designed and fabricated
- An arm capable of manipulating the da Vinci tool about a remote center of motion was designed and fabricated
- Three different boards were designed to interface to the various components on the arm
- A simple kinematics controller Java program was prototyped

The SASHA system has been designed, prototyped, and built. The final product is a standalone arm that is just short of being able to stand statically. After minimal replacements, the arm should be ready for basic research as a proof of concept model. The tool interface accepts any standard da Vinci tool and can measure the torques on the tip of the tool using torque sensors designed by the previous project team. Additionally, the arm should be able to generate sufficient forces and speeds required for surgical procedures.

A low power, 24V .5 amp motor controller was designed and six were fabricated to allow for control of the tool manipulation motors and the linear slide motors. Position control using the encoders and beam break sensors has been successfully demonstrated. These can also successfully receive position commands based on their address and report back their current position.

A high power, 24V 20 amp motor controller was designed and fabricated to allow for control of the gross positioning of the tool in 2 axis. This controller has been tested to verify that it can drive the motor in either direction as well release the brake on the motor.

A strain gauge interface was also designed and fabricated to allow for the strain gauges to be reported back to the kinematics controller, as well as to allow for the tool information to be sent back to the kinematics controller. It was verified that this controller can be programmed.

A simple Java kinematics controller which is able to communicate with the other boards through a USB to RS485 adapter was written. This is able to send and receive position commands by address from the low power motor controllers.

These accomplishments should allow for new group to continue this project. Most of the pieces are in place to be able to control the arm with the haptic controller such as the PHANTOM Desktop.

Future Work

There are a number of different goals for this project in the future. In the near future, the modifications and additional development mentioned in each of the individual components subsections should be implemented. These describe what the next steps in completing this project would be and what modifications would improve the project in terms of ease of use and robustness.

Although the current iteration of SASHA should be able to be used as a basic haptics and telesurgery research device, it would benefit greatly from a further design iteration. Better construction materials and techniques would greatly improve the stiffness and aesthetics of SASHA.

The ultimate goal for this system is for it to be used in haptics and telesurgery research. To do this, the arm should be controlled with a haptic controller such as the PHANTOM Desktop. Since this has only three degrees of force feedback, one of the area's that should be researched with force feedback is how the forces on each joint should be mapped back to the user. It may be that forces in certain axis are more useful than others. Different rates for the force feedback should also be experimented with this, since slower rates could adversely affect surgery. Telesurgery and the delays associated with it are also of interest, and artificially inserting delays to see what is acceptable for control both with and without haptics should be tested.

One of the alternate potential uses of this arm would be as a complement to the da Vinci when performing surgeries. It would be worthwhile to take a further iteration of this arm to the hospital to see how it would fit on the operating table with a da Vinci. Since the fourth da Vinci arm is difficult to position, it may be that a standalone arm would be useful in certain operations. However, the next iteration of the arm may benefit from a decreased scope so that the research aspect of the arm is placed into focus. With a primarily research focus, the size of the arm can be greatly reduced and simplified. Once a suitable research platform has been thoroughly developed, it will be a natural progression towards adapting the system to surgical applications.

Works Cited

Berkelman, P., & Ma, J. (2009). A Compact Modular Teleoperated Robotic System for Laparoscopic Surgery. *The International Journal of Robotics Research*, 1198-1215.

Borden, L., Kozlowski, P., Porter, C., & Corman, J. (2007). Mecahnical failure rate of da Vinci robotic system. *Can J Urol.*, 3499-3501.

Force Dimension. (2011). *Force Dimension Website*. Retrieved 2011 April, from http://www.forcedimension.com/

Hannaford, B. e. (2009). *Evaluation of RAVEN Surgical Telerobot during the NASA*. Retrieved September 2010, from https://www.ee.washington.edu/techsite/papers/documents/

Hannaford, B., & Okamura, A. M. (2008). Haptics. In *Springer Handbook of Robotics* (pp. 719-739). Springer.

Institute of Robotics and Mechatronics. (2010). *MIRO / KineMedic*. Retrieved April 2011, from http://www.dlr.de/rm-neu/en/desktopdefault.aspx/

Institute of Robotics and Mechatronics. (2010). *MiroSurge - Telemanipulation in Minimally Invasive Surgery*. Retrieved April 2011, from http://www.dlr.de/rm/en/desktopdefault.aspx/tabid-3835/

Intuitive Surgical. (2010). *Intuitive Surgical Company Profile*. Retrieved March 2011, from http://www.intuitivesurgical.com/company/profile.html

Intuitive Surgical. (2010). *The da Vinci Surgical System*. Retrieved March 2011, from http://www.intuitivesurgical.com/products/davinci_surgical_system/

Kay, S. (2004). *Remote Surgery*. Retrieved 9 13, 2010, from pbs.org: http://www.pbs.org/wnet/innovation/episode7_essay1.html

Kitagawa, M., Okamura, A., Bethea, B., Gott, V., & Baumgartner, W. A. (2002). Analysis of Suture anipulation Forces for Teleoperation with Force Feedback. *Medical Image Computing and Computer-Assisted Intervention*, 155-162.

Kuebler, B., Seibold, U., & Hirzinger, G. (2005). Development of actuated and sensor integrated forceps for minimally invasive robotic surgery. *Int J Medical Robotics and Computer Assisted Surgery*, 96-107.

Lafranco, A. R. (2004, January). Robotic Surgery: A Current Perspective. *Annals of Surgery*, pp. 14-21.

Marchese, A., & Hoyt, H. (2010). *Force Sensing and Haptc Feedback for Robotics Telesurgery.* Worcester MA: Worcester Polytechnic Institute.

Marescaux, J., Leroy, J., Gagner, M., Rubino, F., Mutter, D., Vix, M., et al. (2001). Transatlantic robot-assisted telesurgery. *nature*, 379-380.

Murphy, D. G., Challacombe, B. J., & Costello, A. J. (2008). Outcomes after robot-assisted laparoscopic radical prostatectomy. *Asian Journal of Andrology*, 94-99.

Parker, W. H. (2010, March 18). *Laparoscopic and Robotic Myoectomy*. Retrieved April 25, 2011, from http://www.fibroidsecondopinion.com/laparoscopic-myomectomy/

SECS Inc. (n.d.). *Design Problem Servomechanism Description.* Retrieved 4 27, 2011, from SECS Inc.: http://www.secsinc.com/pdf/245-264R.pdf

Shimachi, S., Hirunyanitiwatna, S., Fujiwara, Y., Hashimoto, A., & Hakozaki, Y. (2008). Adapter for contact force sensing of the da Vinci robot. *The International Journal of Medical Robotics and Computer Assisted Surgery*, 121-130.

van den Bedem, L. e. (2008). Design of Slave Robot for Laparoscopic and Thoracoscopic Surgery. *20th International Conference of Society for Medical Innovation and Technology.* Vienna.

Appendix A: Low Power Motor Controller

Bill of Materials

Footprint	Comment	LibRef	Designator	Description	Quantity	Supplier 1	Supplier Part Number 1	Supplier Unit Price 1	Supplier Subtotal 1
RESC2012M	.01uF Capacitor 0805	Cap	C1	Capacitor	1	Digi-Key	587-1113-1-ND	0.53	$ 0.53
RESC1608L	.1uF Capacitor 0603	Cap	C2, C3, C5, C8, C11, C12, C13, C14, C17	Capacitor	9	Digi-Key	587-1258-1-ND	0.18	$ 1.62
RESC2012M	2.2uF Capacitor 0805	Cap	C4, C9, C10, C15, C16	Capacitor	5	Digi-Key	445-3464-1-ND		
RESC3225L	100uF Capacitor 1210	Cap	C6	Capacitor	1	Digi-Key	490-3390-1-ND	1.45	$ 1.45
RESC2012M	10uF Capacitor 0805	Cap	C7	Capacitor	1	Digi-Key	PCC2300CT-ND		
DIOM5226X23N	D Schottky	D Schotky	D1	Schottky Diode	1	Digi-Key	B240A-FDICT-ND	0.58	$ 0.58
RESC1608L	BLUE LED	LED3	D2	Typical BLUE SiC LED	1	Digi-Key	511-1589-1-ND	0.66	$ 0.66
INDP101101X48N	Inductor 100 uH	Inductor 100 uH	L1		1	Digi-Key	445-3825-1-ND	1.8	$ 1.80
HDR1X4	Header 4	Header 4	P1	Header, 4-Pin	1	Digi-Key	3M9449-ND	0.17	$ 0.17
HDR2X3	Header 3X2	Header 3X2	P2, P3	Header, 3-Pin, Dual row	2	Digi-Key	3M9459-ND	0.26	$ 0.52
HDR2X7	Header 7X2	Header 7X2	P4	Header, 7-Pin, Dual row	1	Digi-Key	S9170-ND	0.34	$ 0.34
RESC3225L	.1 1% 1210	Res3	R1, R6	Resistor	2	Digi-Key	RHM.10SCT-ND		
RESC1608L	10K 1% 0603	Res3	R2, R10, R15, R16,	Resistor	7	Digi-Key	P10.0KHCT-ND	0.04	$ 0.28

			R18, R23, R24						
RESC1608L	3.16K 1% 0603	Res3	R3	Resistor	1	Digi-Key	P3.16KHCT-ND	0.04	$ 0.04
RESC1608L	2.2K 0603	Res3	R4, R9, R22	Resistor	3	Digi-Key	RMCF0603JT2K20CT-ND	0.02	$ 0.06
RESC1608L	100 0603	Res3	R5	Resistor	1	Digi-Key	RMCF0603JT100RCT-ND	0.02	$ 0.02
RESC1608L	16.5K 1% 0603	Res3	R7, R8, R13, R14	Resistor	4	Digi-Key	P16.5KHCT-ND	0.04	$ 0.16
RESC1608L	3.3K 0603	Res3	R11	Resistor	1	Digi-Key	RMCF0603JT3K30CT-ND	0.02	$ 0.02
RESC1608L	33K 0603	Res3	R12	Resistor	1	Digi-Key	RMCF0603JT33K0CT-ND	0.02	$ 0.02
RESC1608L	20K 0603	Res3	R17, R19	Resistor	2	Digi-Key	RMCF0603JT2K20CT-ND	0.02	$ 0.04
RESC1608L	4.7k 0603	Res3	R20, R21	Resistor	2	Digi-Key	RMCF0603JT4K70CT-ND	0.02	$ 0.04
SOIC127P600X175-8N	TPS5410	TPS5410	U1		1	Digi-Key	296-20787-5-ND	5.46	$ 5.46
TSOP65P490X110-8N	INA170	INA170	U2, U7		2	Digi-Key	INA170EA/2K5CT-ND	3.33	$ 6.66
SOT95P280X145-5N	REG113	REG113	U3		1	Digi-Key	REG113NA-3.3/3KCT-ND	3.15	$ 3.15
SOIC127P600X175-8N	SN65HVD11	SN65HVD11	U4		1	Digi-Key	296-12645-5-ND	4.23	$ 4.23
SOIC127P1030X265-20N	L293D	L293D	U5		1	Digi-Key	497-2937-1-ND	3.78	$ 3.78
TSQFP50P1200X1200X105-64M	TMS320F2803x	TMS320F2803x	U6		1				
					55				$ 31.63

Schematics

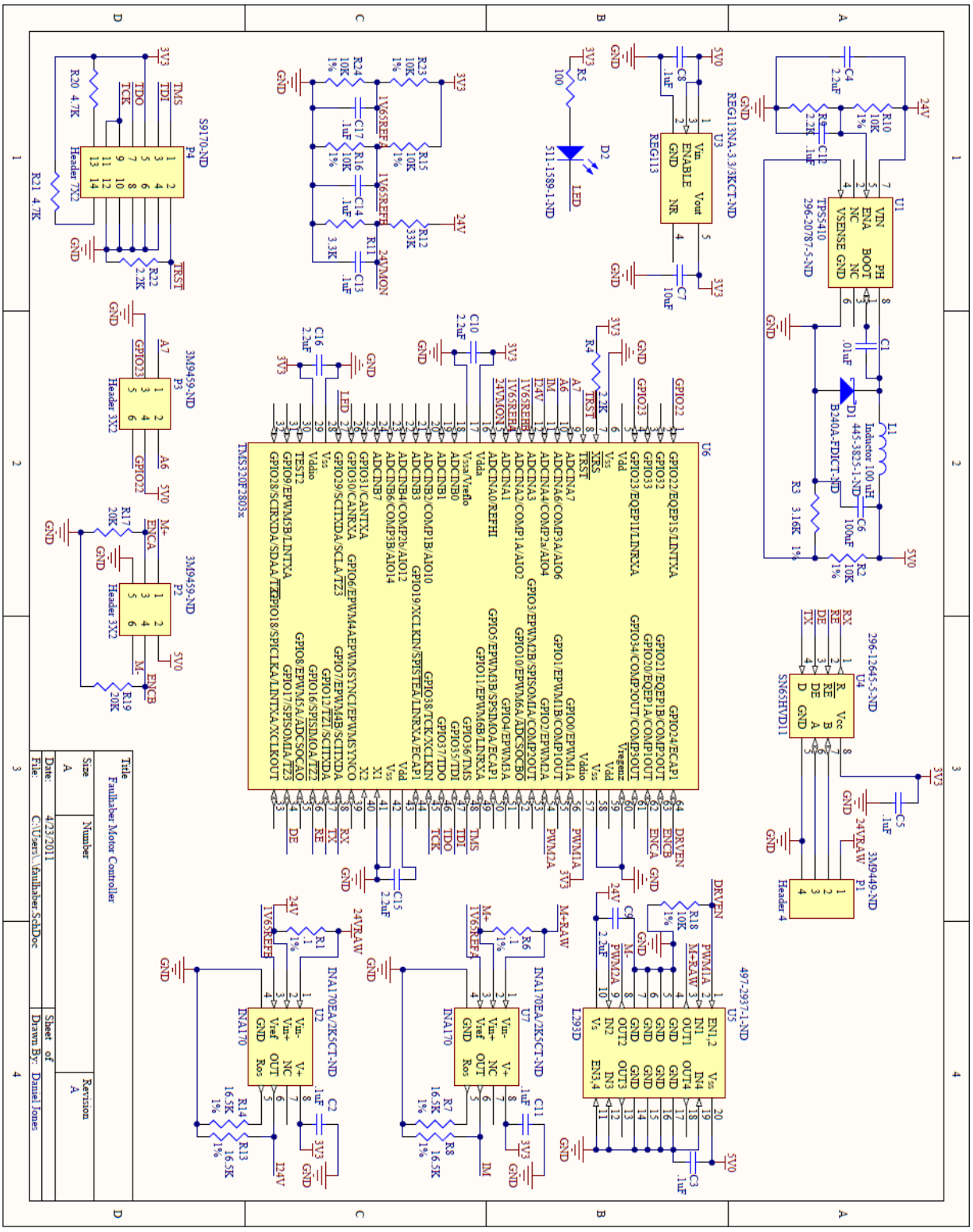

PCB Layout

Top layer:

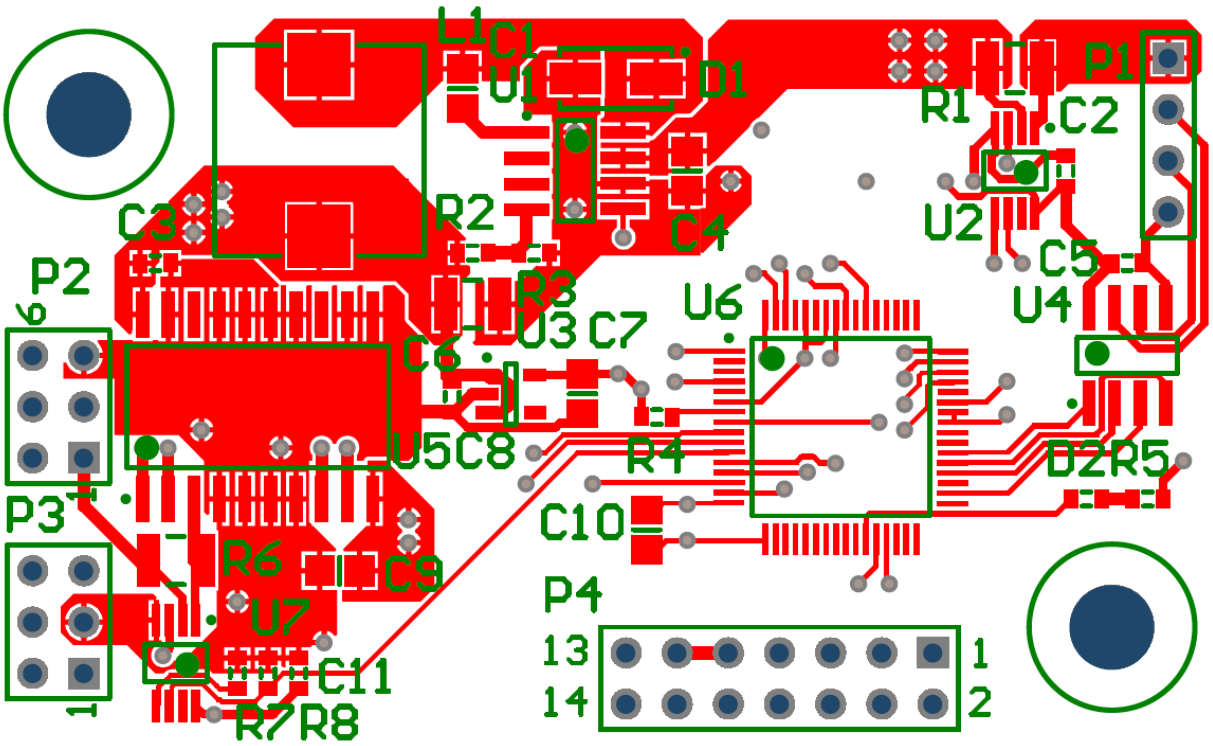

Ground Plane:

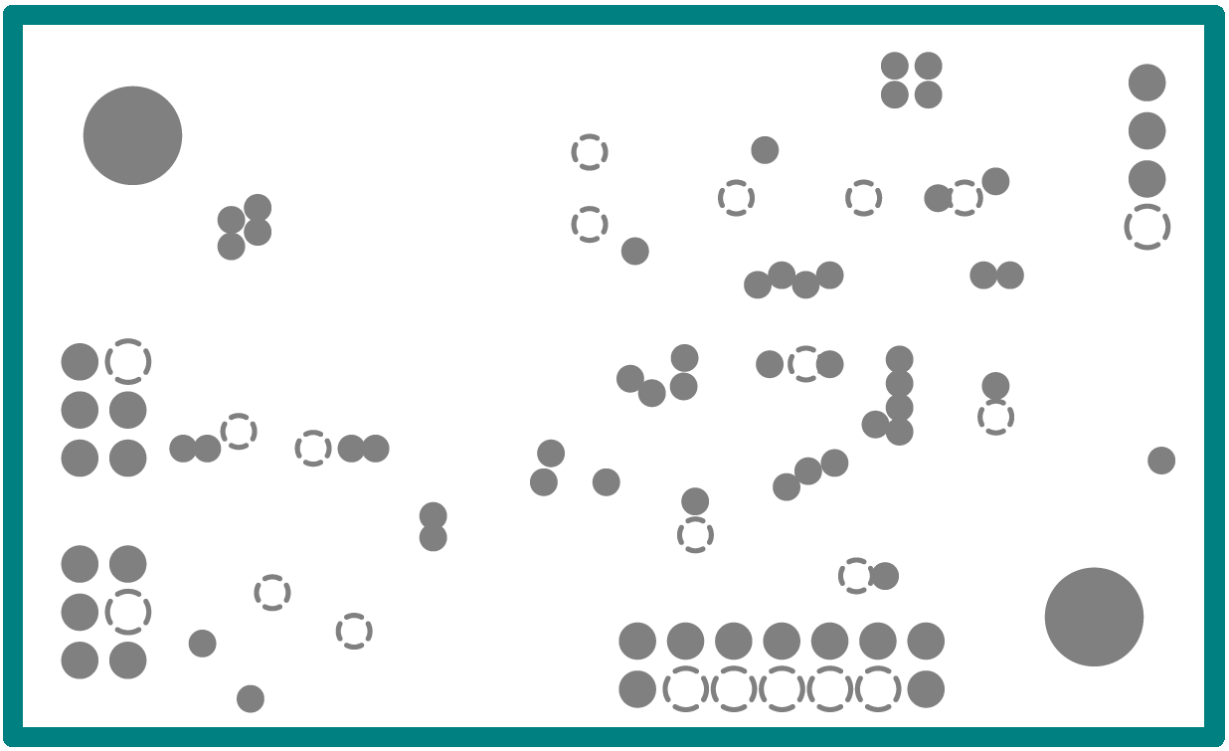

Power layer:

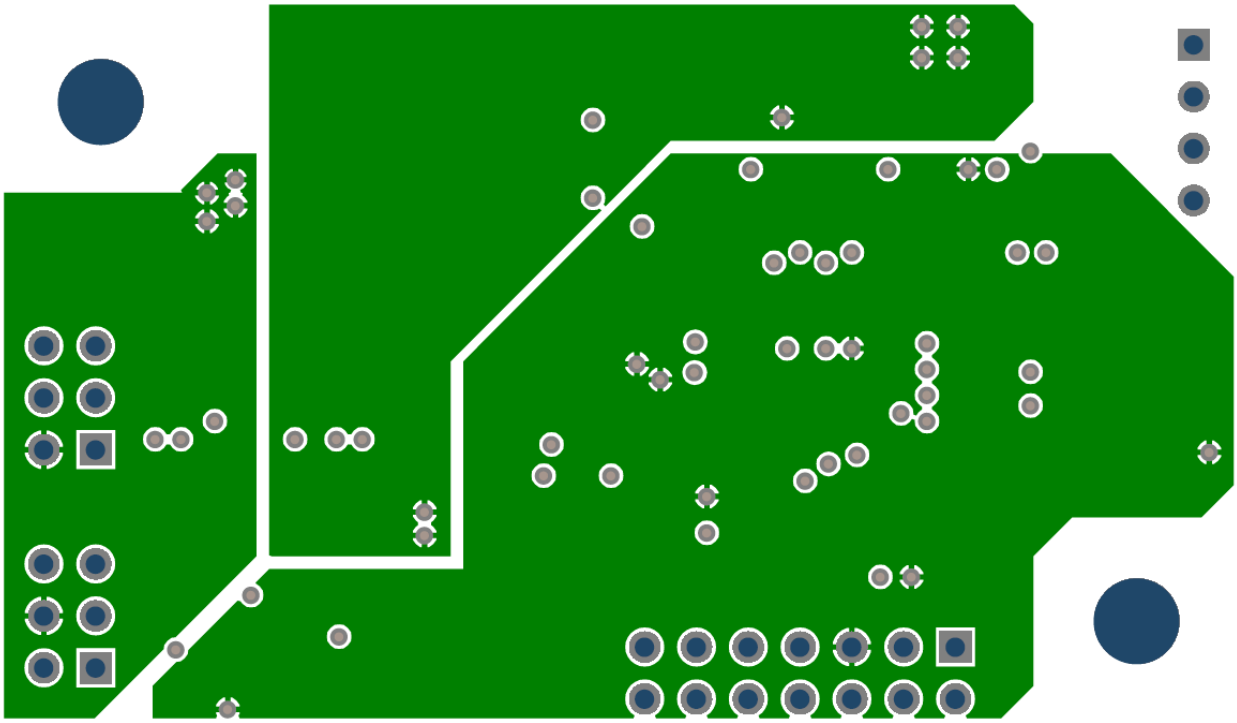

Bottom layer:

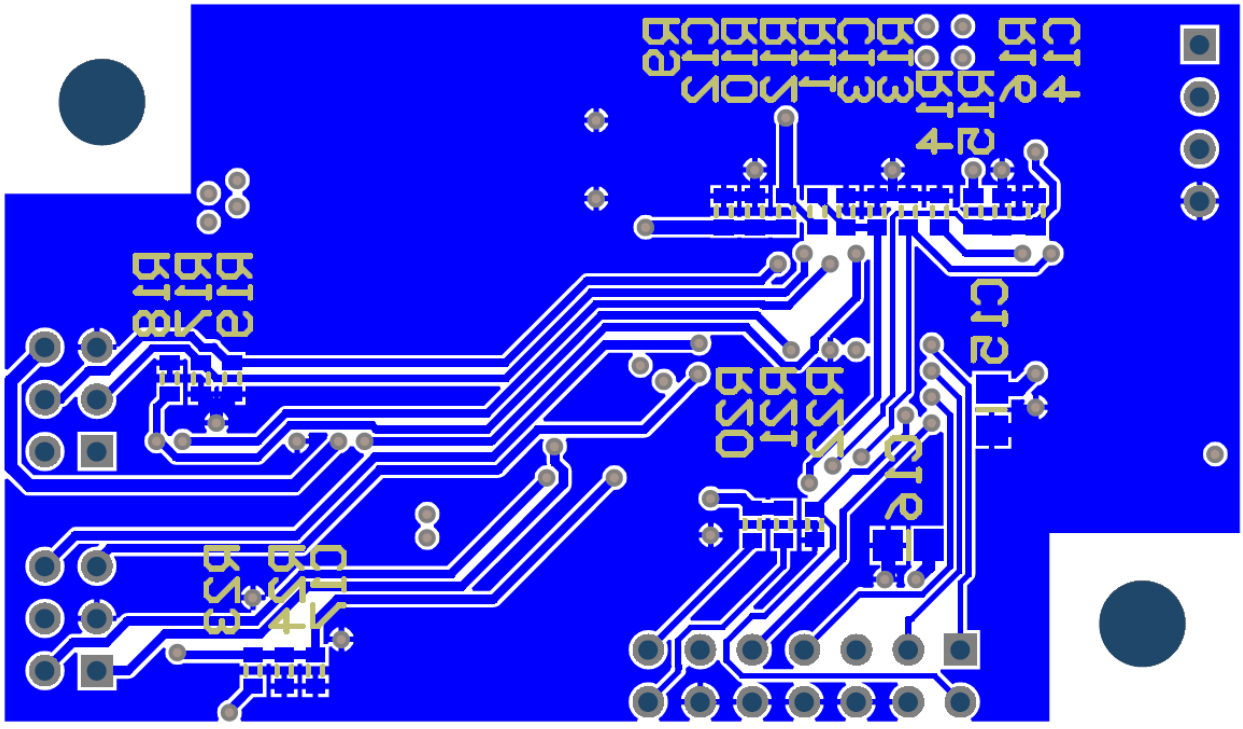

Appendix B: High power Motor Controller

Bill of Materials

Footprint	Comment	LibRef	Designator	Description	Quantity	Supplier 1	Supplier Part Number 1	Supplier Unit Price 1	Supplier Subtotal 1
RESC3225L	100uF Capacitor 1210	Cap	C1	Capacitor	1	Digi-Key	490-3390-1-ND	1.45	$ 1.45
RESC2012M	2.2uF Capacitor 0805	Cap	C2, C3, C11, C14, C25, C26	Capacitor	6	Digi-Key	445-3464-1-ND		
RESC2012M	.01uF Capacitor 0805	Cap	C4	Capacitor	1	Digi-Key	587-1113-1-ND	0.53	$ 0.53
RESC1608L	.1uF Capacitor 0603	Cap	C5, C6, C7, C8, C10, C13, C15, C16, C17, C18, C19, C20, C23, C24, C27	Capacitor	15	Digi-Key	587-1258-1-ND	0.11	$ 1.70
RESC2012M	10uF Capacitor 0805	Cap	C9	Capacitor	1	Digi-Key	PCC2300CT-ND		
RESC1608L	.47uF Capacitor 0603	Cap	C12	Capacitor	1	Digi-Key	445-3456-1-ND		
INDP103103X103N	330uF Electrolytic Capacitor	Electrolytic Capacitor	C21, C22		2	Digi-Key	565-2122-1-ND		
RESC1608L	BLUE LED	LED3	D1	Typical BLUE SiC LED	1	Digi-Key	511-1589-1-ND	0.66	$ 0.66
DIOM5226X23N	D Schottky	D Schottky	D2	Schottky Diode	1	Digi-Key	B240A-FDICT-ND	0.58	$ 0.58
INDP101101X48N	Inductor 100 uH	Inductor 100 uH	L1		1	Digi-Key	445-3825-1-ND	1.8	$ 1.80
HDR2X7	Header 7X2	Header 7X2	P1	Header, 7-Pin, Dual row	1	Digi-Key	S9170-ND	0.34	$ 0.34

HDR2X3	Header 3X2	Header 3X2	P2	Header, 3-Pin, Dual row	1	Digi-Key	3M9459-ND	0.26	$ 0.26
Molex - 10 Pin	Molex - 10 Pin	Molex - 10 Pin	P3		1	Digi-Key	WM3804-ND	2.22	$ 2.22
Molex - 4 PIN	Molex - 4 Pin	Molex - 4 Pin	P4		1	Digi-Key	WM3801-ND	1.21	$ 1.21
TO-252AA	IRFR1205	IRFR1205	Q1, Q2, Q3, Q4, Q5, Q6	HEXFET Power MOSFET	6	Digi-Key	IRFR1205PBFCT-ND	1.56	$ 9.36
RESC1608L	3.16K 1% 0603	Res3	R1	Resistor	1	Digi-Key	P3.16KHCT-ND	0.04	$ 0.04
RESC1608L	10K 1% 0603	Res3	R2, R5, R16	Resistor	3	Digi-Key	P10.0KHCT-ND	0.04	$ 0.12
RESC1608L	100 0603	Res3	R3	Resistor	1	Digi-Key	RMCF0603JT100RCT-ND	0.02	$ 0.02
RESC1608L	2.2K 0603	Res3	R4, R6, R11, R12, R15, R21	Resistor	6	Digi-Key	RMCF0603JT2K20CT-ND	0.02	$ 0.12
RESC1608L	3.3K 0603	Res3	R7, R13, R14, R20	Resistor	4	Digi-Key	RMCF0603JT3K30CT-ND	0.02	$ 0.08
RESC1608L	33K 0603	Res3	R8	Resistor	1	Digi-Key	RMCF0603JT33K0CT-ND	0.02	$ 0.02
RESC1608L	4.7k 0603	Res3	R9, R10	Resistor	2	Digi-Key	RMCF0603JT4K70CT-ND	0.02	$ 0.04
RESC1608L	1 0603	Res3	R17, R18, R19, R22, R23, R24	Resistor	6	Digi-Key	RMCF0603JT1R00CT-ND	0.02	$ 0.12
SOIC127P600X175-8N	TPS5410	TPS5410	U1		1	Digi-Key	296-20787-5-ND	5.46	$ 5.46
TSQFP50P1200X1200X105-64M	TMS320F2803x	TMS320F2803x	U2		1				
SOIC127P600X175-8N	SN65HVD11	SN65HVD11	U3		1	Digi-Key	296-12645-5-ND	4.23	$ 4.23
TSOP63P600X150-24L	ACS709	ACS709	U4, U7		2	Digi-	620-1337-1-	4.24	$ 8.48

						Key	ND		
SOT95P280X145-5N	REG113	REG113	U5		1	Digi-Key	REG113NA-3.3/3KCT-ND	3.15	$ 3.15
TSQFP50P900X900X160_HS-48L	A4935	A4935	U6		1	Digi-Key	620-1300-1-ND	7.42	$ 7.42
					71				$ 49.41

Schematic

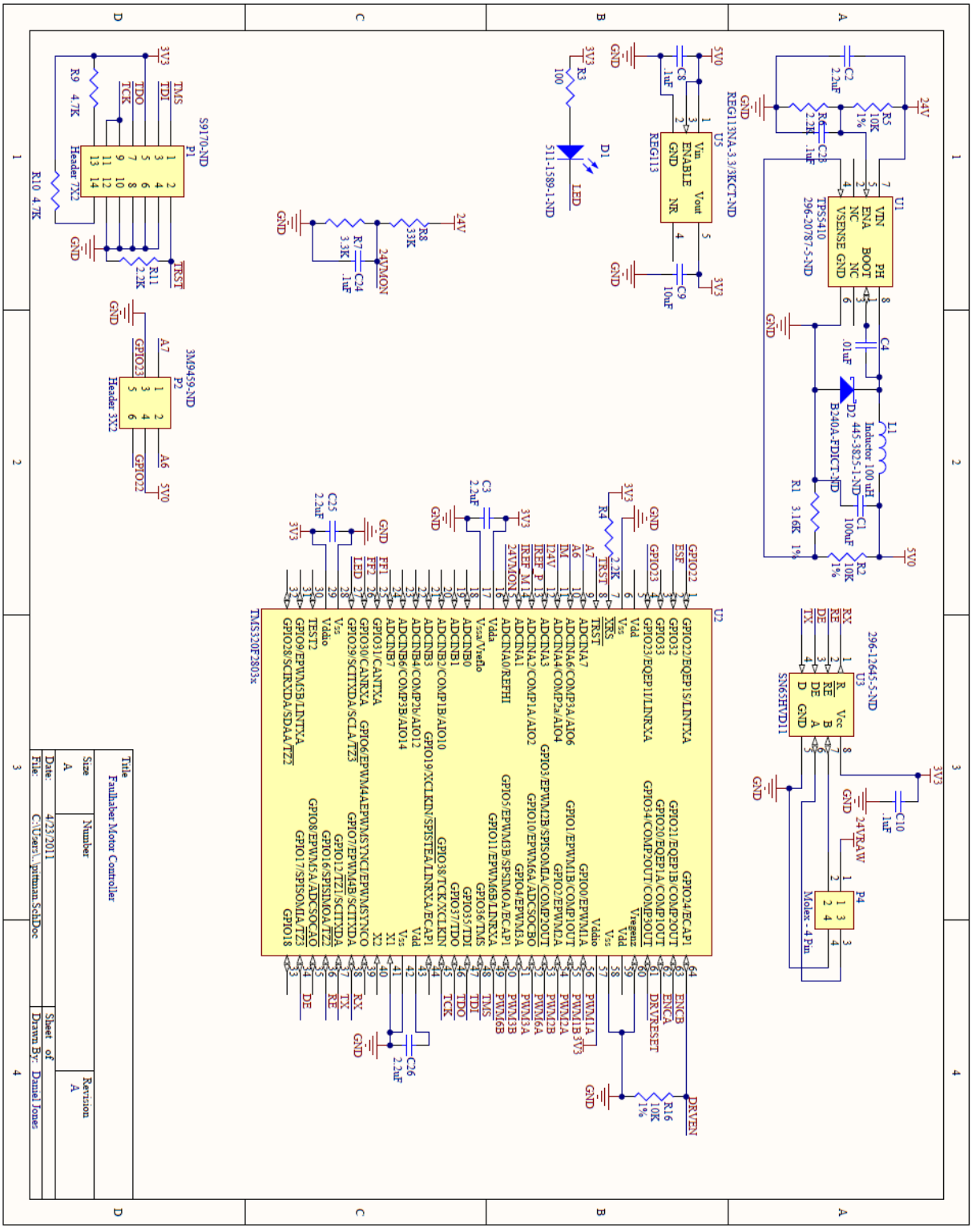
Title
Faulhaber Motor Controller
Size
A
Number
Revision
A
Date: 4/23/2011
Sheet of
File: C:\Users\...\pittman.SchDoc
Drawn By: Daniel Jones
U1
TPS5410
296-2078-5-ND
U2
TMS320F2803x
U3
SN65HVD11
296-12645-5-ND
U5
REG113
REG113NA-3.3/3KCT-ND
D1
511-1589-1-ND
D2
B340A-FDICT-ND
L1
Inductor 100 uH
445-3825-1-ND
P1
S9170-ND
P2
3M9459-ND
P4
Molex - 4 Pin
24V
5V0
3V3
GND
DRVEN
ENCB
ENCA
DRVRESET
PWM1A
PWM1B
PWM2A
PWM2B
PWM3A
PWM3B
PWM6A
PWM6B
TMS
TDI
TDO
TCK
RX
TX
RE
DE
TRST
24VMON

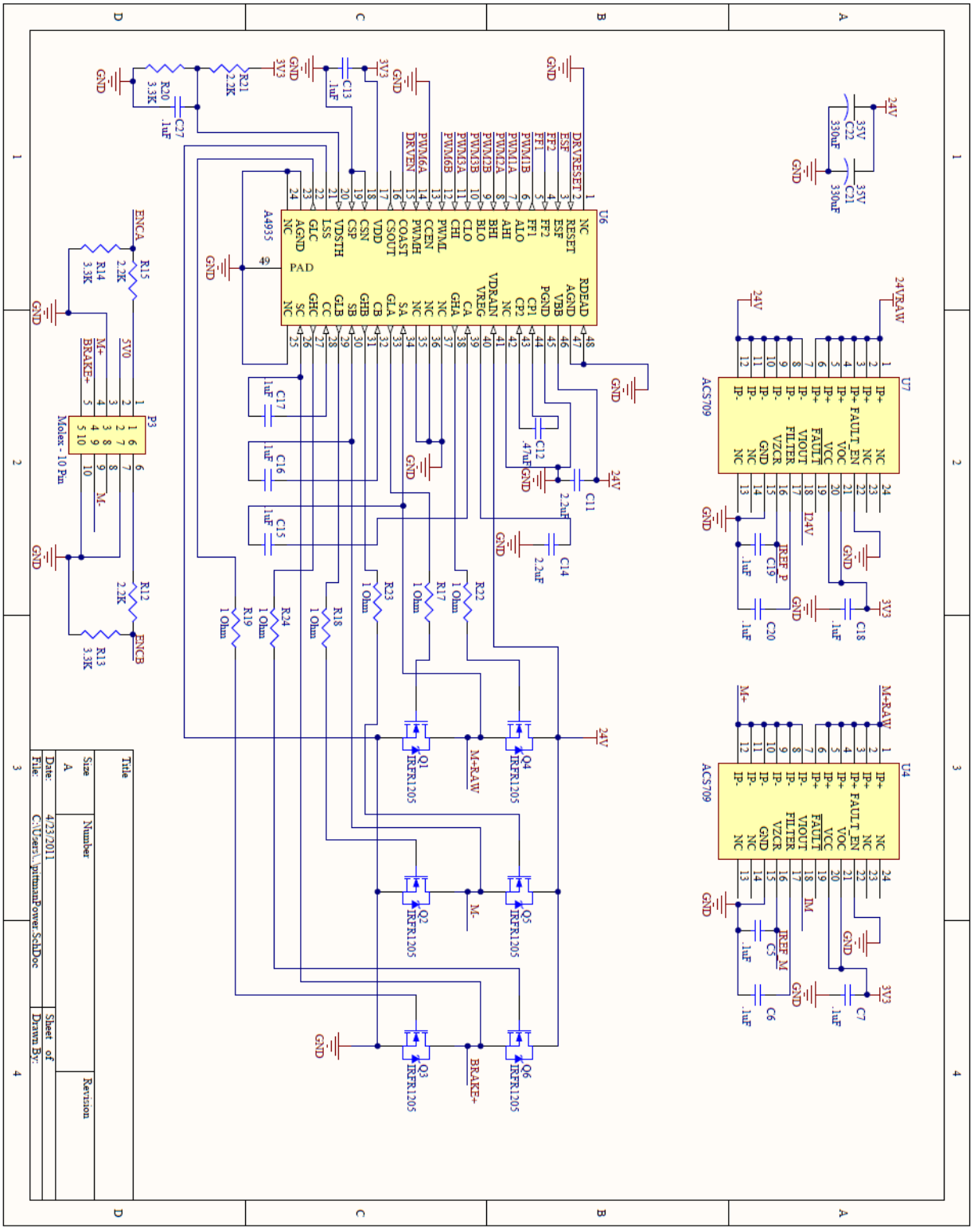
24V
35V
C22
330uF
C21
330uF
24VRAW
U7
ACS709
IP+
IP-
NC
FAULT_EN
VIOC
VCC
FAULT
VIOUT
FILTER
VZCR
GND
I24V
IREF_P
C19
.1uF
C20
C18
3V3
M+
M+RAW
U4
IM
IREF_M
C5
C6
C7
24V
DRVRESET
ESF
FF3
FF2
FF1
PWM1B
PWM1A
PWM2A
PWM2B
PWM3B
PWM3A
PWM6B
PWM6A
DRVEN
U6
A4935
PAD
NC
RESET
AGND
VBB
PGND
CP1
CP2
VDRAIN
VREG
CA
GHA
NC
SA
GLA
CB
GHB
SB
GLB
CC
GHC
SC
AGND
GLC
LSS
VDSTH
CSP
CSN
VDD
COAST
CSOUT
CCEN
PWML
PWMH
RDEAD
C27
1uF
R20
3.3K
R21
2.2K
C13
.1uF
C12
.47uF
C11
2.2uF
C14
2.2uF
C17
1uF
C16
1uF
C15
1uF
R22
1 Ohm
R17
1 Ohm
R23
1 Ohm
R18
1 Ohm
R24
1 Ohm
R19
1 Ohm
Q1
IRFR1205
Q2
IRFR1205
Q3
IRFR1205
Q4
IRFR1205
Q5
IRFR1205
Q6
IRFR1205
M+RAW
M-
BRAKE+
ENCA
ENCB
R15
2.2K
R14
3.3K
R12
2.2K
R13
3.3K
5V0
BRAKE+
M-
P3
Molex-10 Pin
Title
Size
A
Number
Revision
Date:
4/23/2011
File:
C:\Users\...putmanaPower.SchDoc
Sheet of
Drawn By:

PCB Layout

Top layer:

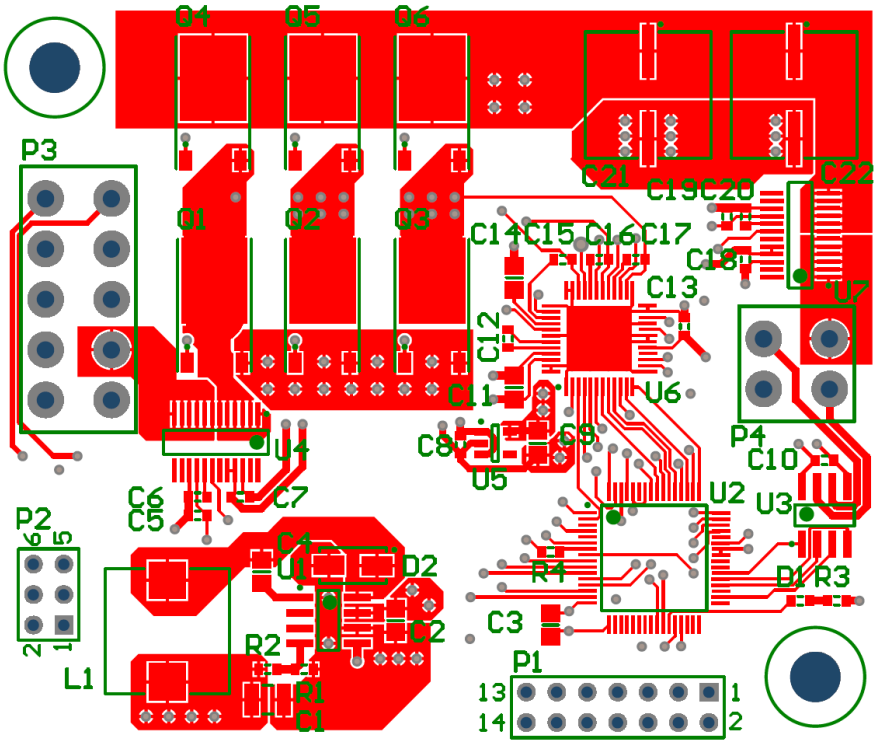

Bottom layer:

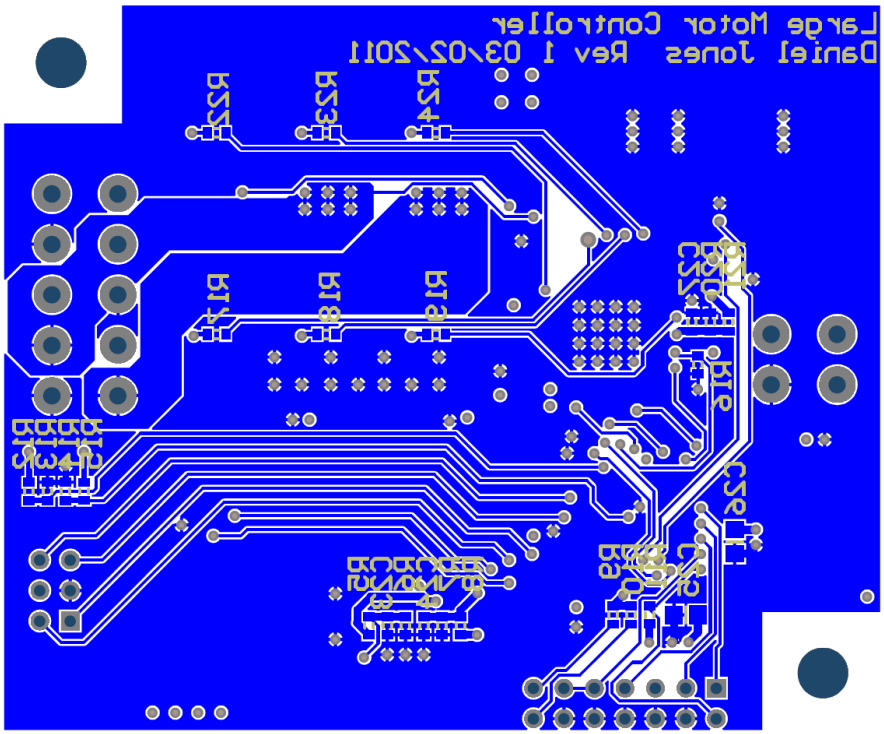

Appendix C: Strain Gauge Interface

Bill of Materials

Footprint	Comment	LibRef	Designator	Description	Quantity	Supplier 1	Supplier Part Number 1	Supplier Unit Price 1	Supplier Subtotal 1
RESC2012M	.01uF Capacitor 0805	Cap	C1	Capacitor	1	Digi-Key	587-1113-1-ND	0.53	$ 0.53
RESC2012M	2.2uF Capacitor 0805	Cap	C2, C4, C19, C20	Capacitor	4	Digi-Key	445-3464-1-ND		
RESC3225L	100uF Capacitor 1210	Cap	C3	Capacitor	1	Digi-Key	490-3390-1-ND	1.45	$ 1.45
RESC1608L	.1uF Capacitor 0603	Cap	C5, C7, C8, C9, C10, C11, C12, C13, C14, C16, C17, C18, C21	Capacitor	13	Digi-Key	587-1258-1-ND	0.11	$ 1.47
RESC2012M	10uF Capacitor 0805	Cap	C6, C15	Capacitor	2	Digi-Key	PCC2300CT-ND		
DIOM5226X23N	D Schottky	D Schottky	D1	Schottky Diode	1	Digi-Key	B240A-FDICT-ND	0.58	$ 0.58
RESC1608L	BLUE LED	LED3	D2	Typical BLUE SiC LED	1	Digi-Key	511-1589-1-ND	0.66	$ 0.66
INDP101101X48N	Inductor 100 uH	Inductor 100 uH	L1		1	Digi-Key	445-3825-1-ND	1.8	$ 1.80
HDR1X4	Header 4	Header 4	P1, P2, P3, P4, P8	Header, 4-Pin	5	Digi-Key	3M9449-ND	0.17	$ 0.85
HDR2X3	Header 3X2	Header 3X2	P5	Header, 3-Pin, Dual row	1	Digi-Key	3M9459-ND	0.26	$ 0.26
HDR1X2	Header 2	Header 2	P6	Header, 2-Pin	1				

HDR2X7	Header 7X2	Header 7X2	P7	Header, 7-Pin, Dual row	1	Digi-Key	S9170-ND	0.34	$ 0.34
RESC1608L	10K 1% 0603	Res3	R1, R25, R31, R32	Resistor	4	Digi-Key	P10.0KHCT-ND	0.04	$ 0.16
RESC1608L	3.16K 1% 0603	Res3	R2	Resistor	1	Digi-Key	P3.16KHCT-ND	0.04	$ 0.04
RESC1608L	2.2K 0603	Res3	R3, R11, R22, R26	Resistor	4	Digi-Key	RMCF0603JT2K20CT-ND	0.02	$ 0.08
RESC3225L	.1 1% 1210	Res3	R4	Resistor	1	Digi-Key	RHM.10SCT-ND		
RESC1608L	100 0603	Res3	R5	Resistor	1	Digi-Key	RMCF0603JT100RCT-ND	0.02	$ 0.02
RESC1608L	480 0603	Res3	R6, R8, R14, R16	Resistor	4	Digi-Key	P475HCT-ND	0.04	$ 0.16
RESC1608L	1k 0603	Res3	R7, R9, R12, R13, R15, R17, R19, R20	Resistor	8	Digi-Key	P1.00KHCT-ND	0.04	$ 0.32
RESC1608L	3.3K 0603	Res3	R10, R27	Resistor	2	Digi-Key	RMCF0603JT3K30CT-ND	0.02	$ 0.04
RESC1608L	220K 0603	Res3	R18	Resistor	1	Digi-Key	P220KHCT-ND	0.04	$ 0.04
RESC1608L	26.1K 0603	Res3	R21	Resistor	1	Digi-Key	P26.1KHCT-ND	0.04	$ 0.04
RESC1608L	4.7k 0603	Res3	R23, R24	Resistor	2	Digi-Key	RMCF0603JT4K70CT-ND	0.02	$ 0.04
RESC1608L	33K 0603	Res3	R28	Resistor	1	Digi-Key	RMCF0603JT33K0CT-ND	0.02	$ 0.02
RESC1608L	16.5K 1% 0603	Res3	R29, R30	Resistor	2	Digi-Key	P16.5KHCT-ND	0.04	$ 0.08
SOIC127P600-8N	AD620AR	AD620AR	U1, U2, U4, U5	Low-Cost, Low-Power Instrumentation Amplifier	4	Digi-Key	AD620ARZ-REEL7CT-ND	9.17	$ 36.68

SOIC127P600X175-8N-DS2480	DS2480B	DS2480B	U3		1	Digi-Key	DS2480B+-ND	5.55	$ 5.55
TSOP65P490X110-8N	TPS79801	TPS79801	U6		1	Digi-Key	296-24322-1-ND	1.42	$ 1.42
SOIC127P600X175-8N	TPS5410	TPS5410	U7		1	Digi-Key	296-20787-5-ND	5.46	$ 5.46
TSQFP50P1200X1200X105-64M	TMS320F2803x	TMS320F2803x	U8		1				
SOT95P280X145-5N	REG113	REG113	U9		1	Digi-Key	REG113NA-3.3/3KCT-ND	3.15	$ 3.15
TSOP65P490X110-8N	INA170	INA170	U10		1	Digi-Key	INA170EA/2K5CT-ND	3.33	$ 3.33
SOIC127P600X175-8N	SN65HVD11	SN65HVD11	U11		1	Digi-Key	296-12645-5-ND	4.23	$ 4.23
					75				$ 68.80

Schematic

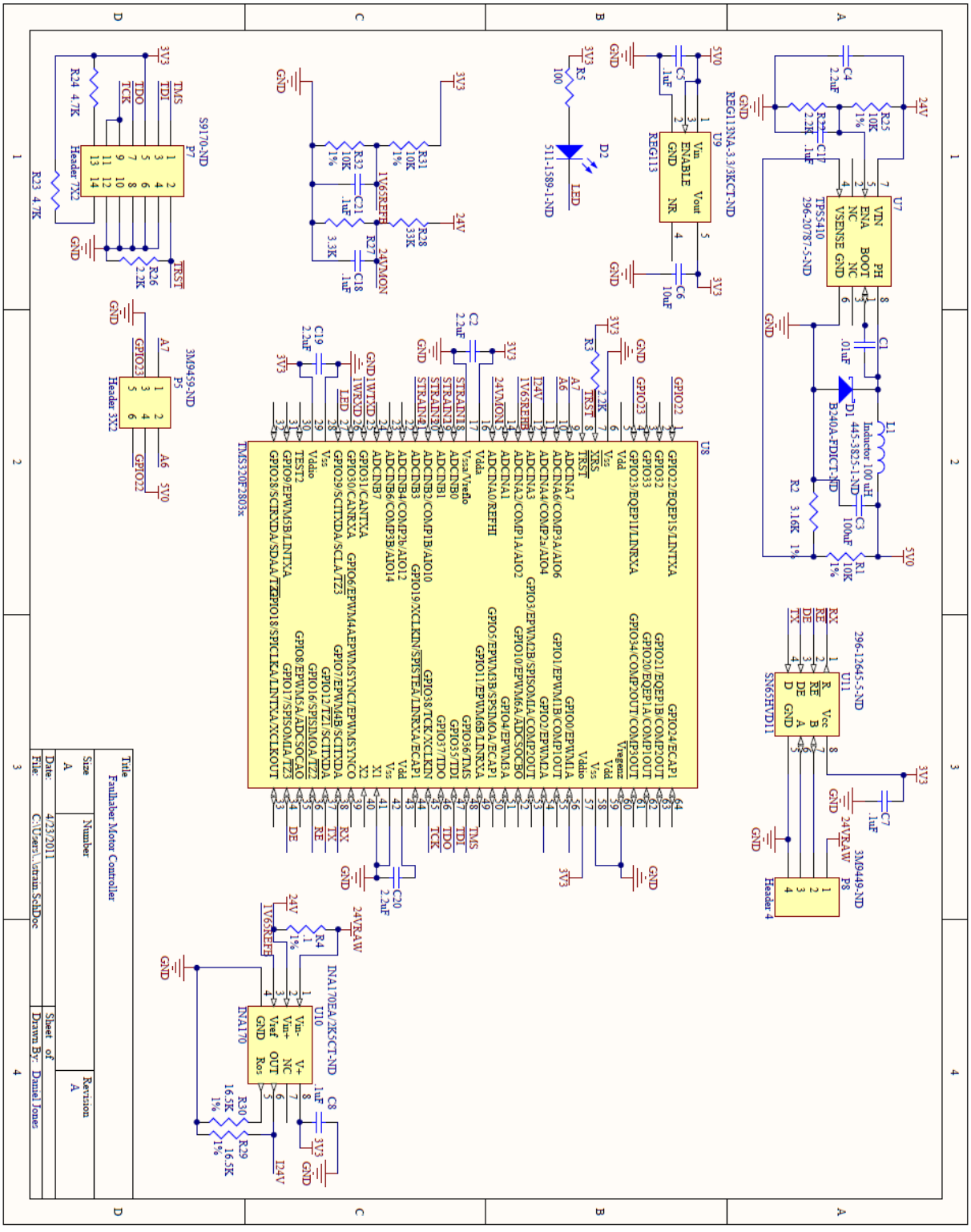
Title
Faulhaber Motor Controller
Size
A
Number
Revision
A
Date: 4/23/2011
Sheet of
File: C:\Users\...\strain.SchDoc
Drawn By: Daniel Jones
TMS320F2803x
REG113NA-3.3/3KCT-ND
TPS54310
296-20787-5-ND
445-3825-1-ND
511-1589-1-ND
SN65HVD11
296-12645-5-ND
S9170-ND
3M9459-ND
3M9449-ND
INA170
INA170EA/2K5CT-ND
24V
5V0
3V3
24VRAW
GND
LED
TMS
TDI
TDO
TCK
TRST
RX
TX
RE
DE

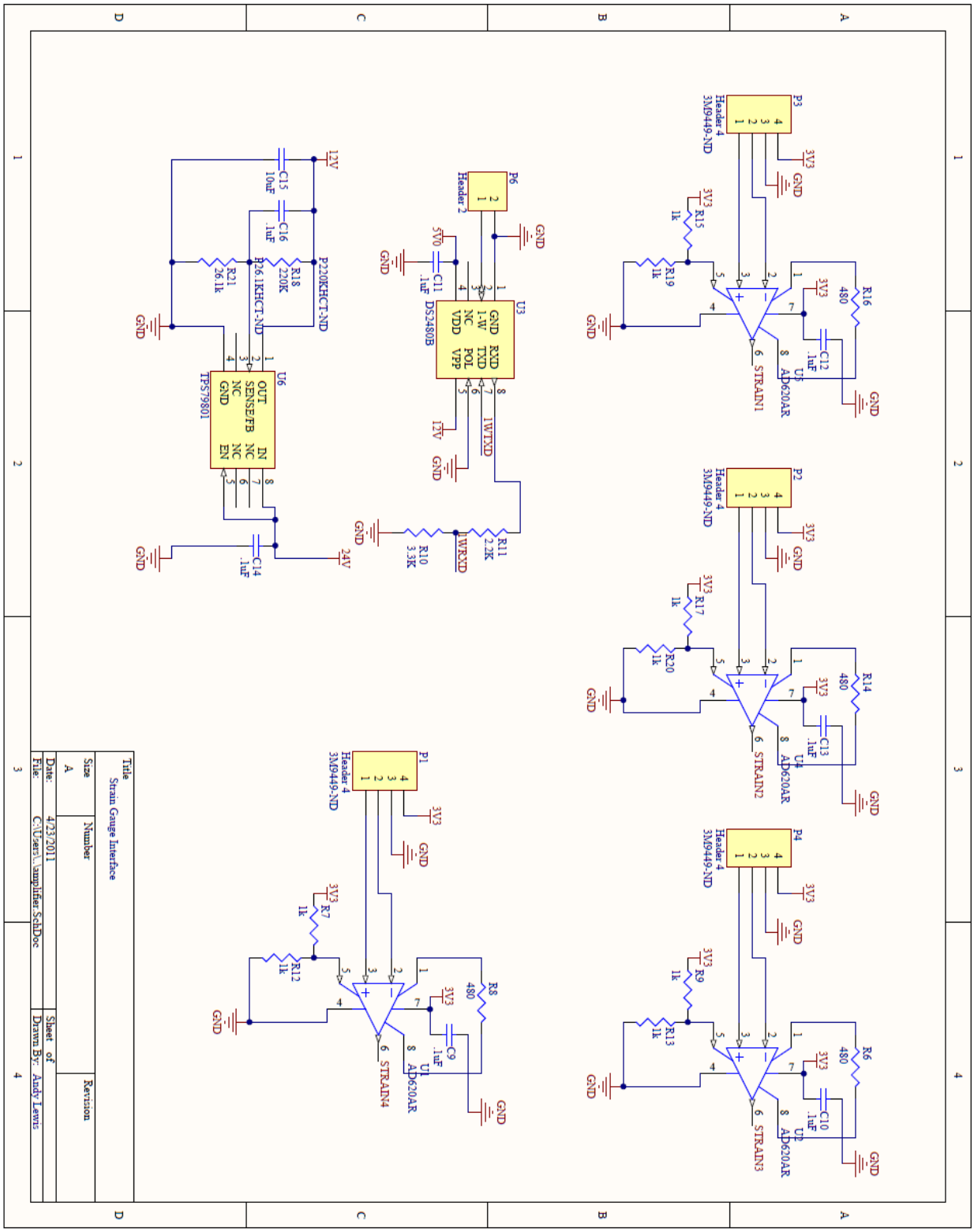
Title
Strain Gauge Interface
Size
A
Number
Revision
Date:
4/23/2011
Sheet of
File:
C:\Users\...mplifier.SchDoc
Drawn By:
Andy Lewis
P3
Header 4
3M9449-ND
P2
P4
P1
P6
Header 2
U3
DS2480B
U5
U4
U2
U1
AD620AR
U6
TPS79801
R16
R14
R6
R8
R15
R17
R9
R7
R19
R20
R13
R12
R18
220K
R21
26.1k
R11
2.2K
R10
3.3K
C15
10uF
C16
.1uF
C11
.1uF
C12
.1uF
C13
.1uF
C10
.1uF
C9
.1uF
C14
.1uF
P220KHCT-ND
26.1KHCT-ND
3V3
5V0
12V
24V
GND
STRAIN1
STRAIN2
STRAIN3
STRAIN4
1WTXD
1WRXD

PCB Layout:

Top layer:

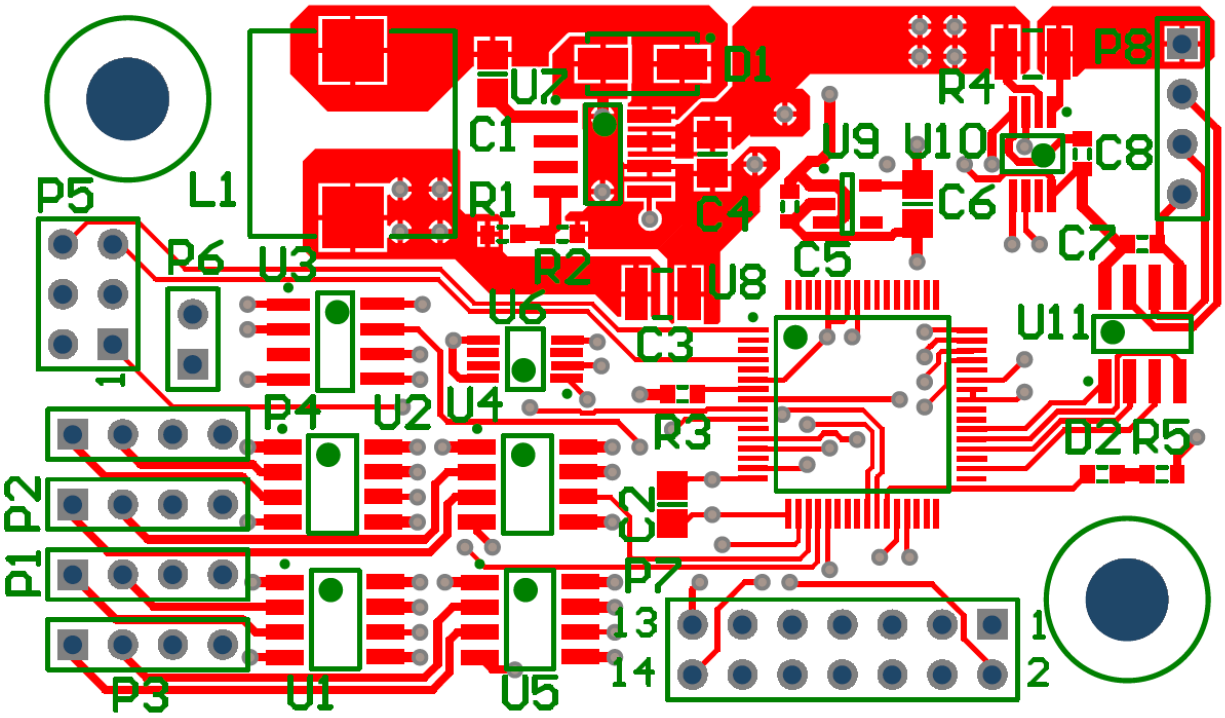

Ground plane:

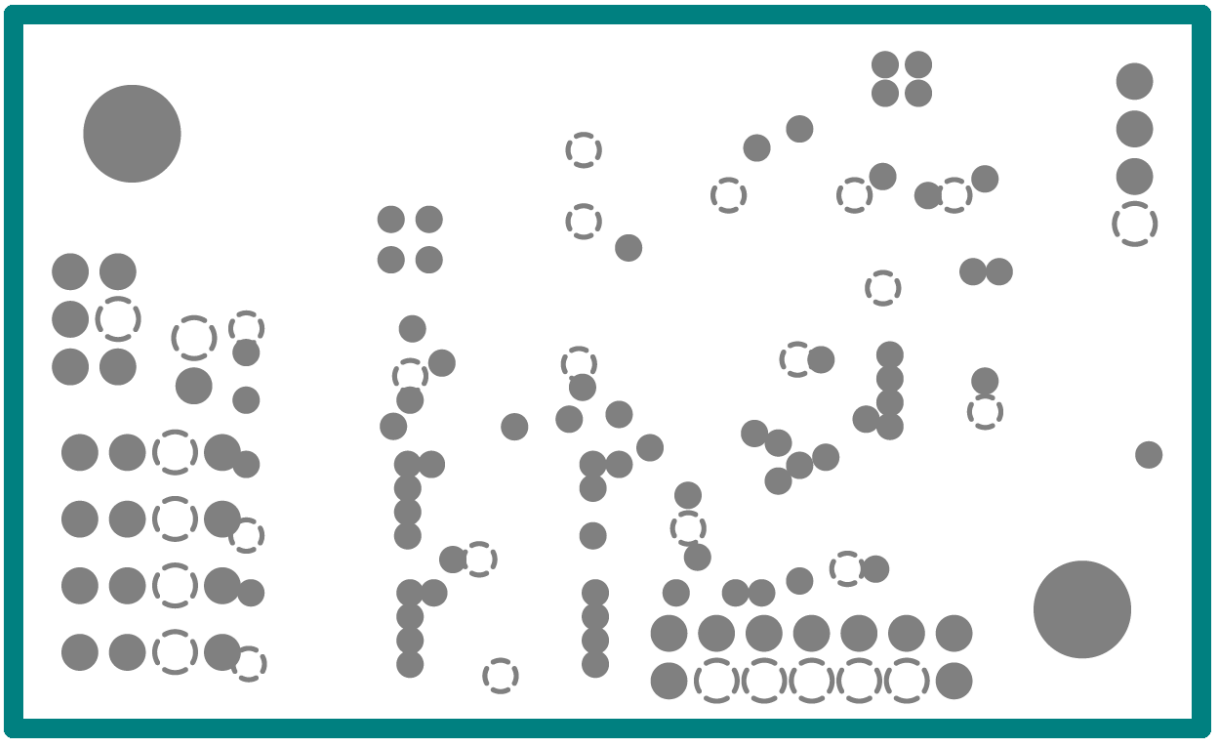

Power layer:

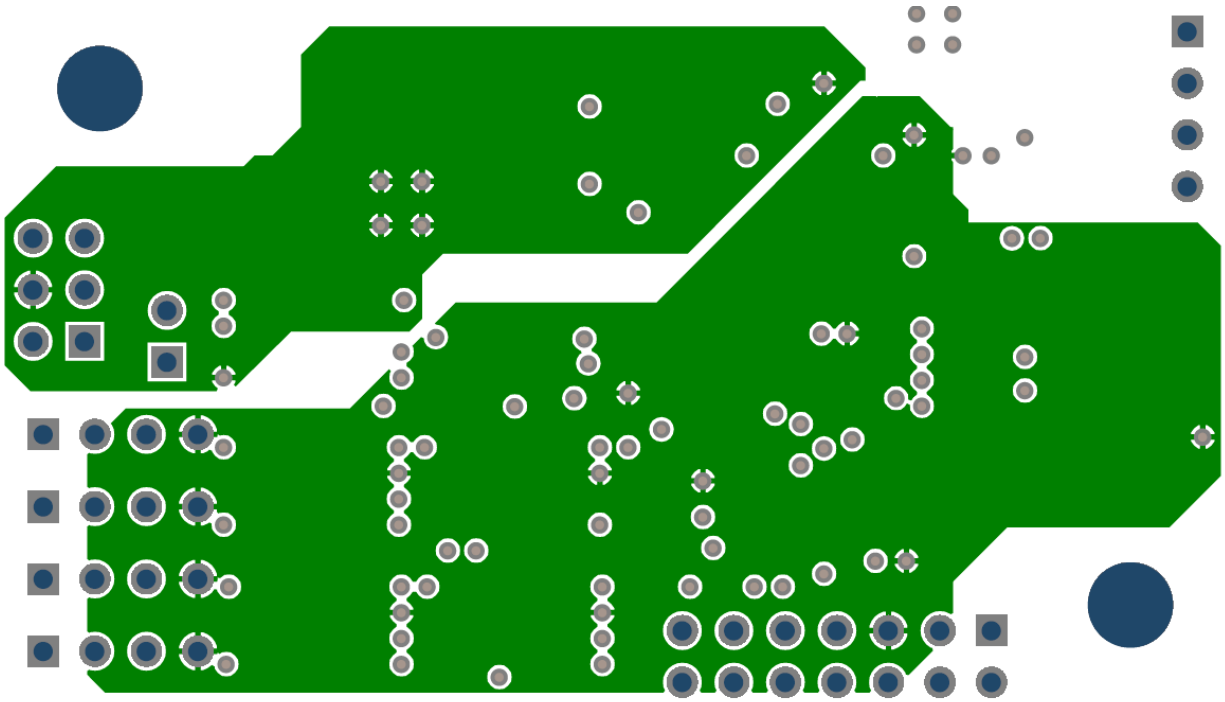

Bottom layer:

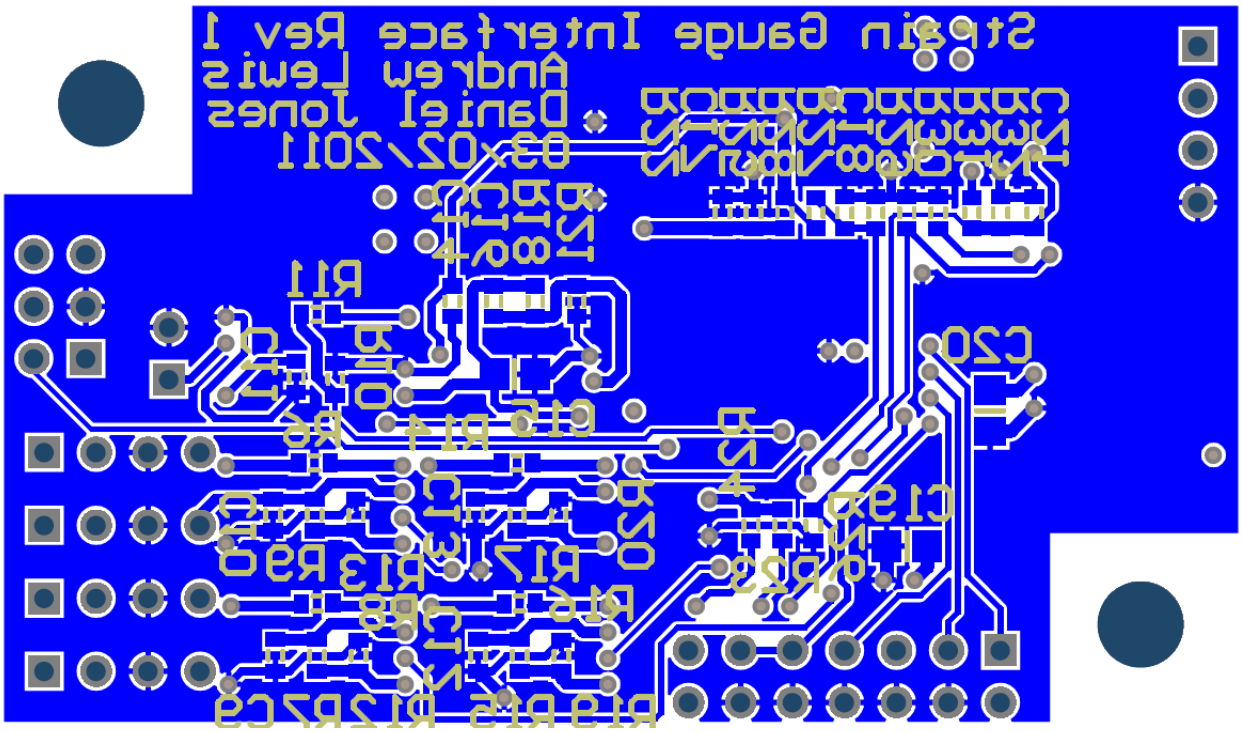

Appendix D: Safe working gear load calculations

Formula and additional information (SECS Inc.):

$$W_t = \frac{S_W F Y}{P} \times \frac{600}{600+V}$$

where

W_t	=	Safe Pitch Line Load, lbs.
S_W	=	Safe Stress,psi
F	=	Gear Tooth Width,inches
Y	=	Lewis Form Factor
P	=	Diametral Pitch
V	=	Pitch Line Velocity, feet per min.

The Lewis form factor, Y is given in the adjacent table. Safe values of S_W for the principle gear materials of this catalog are:

303 Stainless Steel	30,000 psi
2024T4 Aluminum	47,000 psi

The standard Lewis Formula may be slightly modified for convenient calculation of gear torque capacity. Use W_t the safe pitch line loading, in lbs as a starting point.

$$T = N/P \times 1/2 \times W_t \text{ in-lbs}$$

where:

T = Torque

N = Number of Gear Teeth

P = Diametral Pitch

Lewis Form Factor, Y, for Loading Near the Pitch Point fof 20° Full Depth Gear Teeth

NUMBER	Y	FUNCTIONS of Y for TORQUE CALCULATIONS	
		Y x N	Y/N
10	0.201	2.01	0.0201
11	0.226	2.49	0.0205
12	0.245	2.94	0.0204
13	0.261	3.39	0.0201
14	0.276	3.86	0.0197
15	0.289	4.335	0.0193
16	0.295	4.72	0.0184
17	0.302	5.13	0.0178
18	0.308	5.54	0.0171
19	0.314	5.97	0.0165
20	0.320	6.40	0.0160
21	0.327	6.87	0.0156
23	0.333	7.66	0.0145
25	0.339	8.475	0.0136
27	0.349	9.42	0.0129
30	0.358	10.07	0.0119
34	0.371	12.6	0.0109
38	0.383	14.6	0.0101
43	0.396	17.0	0.00921
50	0.408	20.4	0.00816
60	0.421	25.3	0.00702
75	0.434	32.6	0.00579
100	0.446	44.6	0.00466
150	0.459	68.85	0.00306
300	0.471	141.0	0.00157
RACK	0.484		

Sample Mathematica code:

```
sw = 30000;
f = .1875;
y = .308;
rpm = 26.36 * 40 / 15;
teeth = 18;
p = 24;
v = rpm * Pi / 12. * teeth / p;
wt = sw * f * y / p * 600 / (600 + v)
t = teeth / p * .5 * wt / 12
```

Appendix E: Paper Submitted to EMBC 2011

Development of a StandAlone Surgical Haptic Arm (SASHA)

Daniel Jones†, Andrew Lewis†, and Professor Gregory S. Fischer

***Abstract*— When performing telesurgery with commercially available Minimally Invasive Robotic Surgery (MIRS) systems, a surgeon cannot feel the tool interactions that are inherent in traditional laparoscopy. It is proposed that haptic feedback in the control of MIRS systems could improve the speed, safety and learning curve of robotic surgery. To test this hypothesis, a standalone surgical arm capable of manipulating da Vinci tools has been designed and fabricated with the additional ability of providing information for haptic feedback. This arm will be used as a platform for research on the performance of telesurgery as a function of various haptic mappings and latencies.**

I. Introduction

Minimally Invasive Robotic Surgery (MIRS) is currently dominated by Intuitive Surgical's da Vinci system[1]. The first da Vinci system was introduced in 1999, and the most recent da Vinci SI system offers a 3D HD vision system, three robotic surgical arms and another robotic arm for controlling an endoscopic camera[2]. All of the arms attach to a common column that is wheeled to the operating table prior to surgery. A wide variety of interchangeable and disposable tools allows for a wide variety of surgical procedures that would be impossible to perform with traditional laparoscopy. Currently, haptic feedback is not an advertised feature of the da Vinci system.

Following the da Vinci's widespread success, there is a variety of research being performed to develop new MIRS systems. The German Aerospace Center (DLR) has developed its second generation robotic arm (MIRO) that is used in its MiroSurge robotic system[3]. The arms weigh less than 10 kg and, unlike the da Vinci system, can be attached directly to the operating table in order to optimize the workspace of each arm with respect to the others, much like the earlier Zeus system[4]. The MiroSurge system consists of three 7 Degree of Freedom (DoF) MIRO arms: two manipulating laparoscopic tools and another manipulating an endoscopic camera[5]. Force and torque sensors located near the tips of the tools provide feedback that is represented haptically with Force Dimension's Omega.7 haptic controllers. Three translational degrees of haptic feedback are possible with the Omega.7 controller[6]. The ultimate goal in developing this technology is to be able to use the Mirosurge system to operate on a beating heart, thereby eliminating the need and risks of heart/lung machines.

Teleoperation and telesurgery is the ability for surgeons to perform operations remotely, greatly reducing transportation costs as well as allowing a specialist to practice in almost any region of the world. The BioRobotics Lab at the University of Washington is in the process of developing and testing the RAVEN telerobotic system[7], which is specifically aimed at researching the effects of long distances on telesurgery. In 2007, this system was tested in the NASA Extreme Environment Mission Operations (NEEMO) 12 Mission. The system was successfully operated in an underwater lab off the coast of Florida from stations in Ohio, Florida and Washington. Although the RAVEN is currently teleoperated with Sensable's PHANTOM Omni controllers, haptic feedback has not yet been implemented.

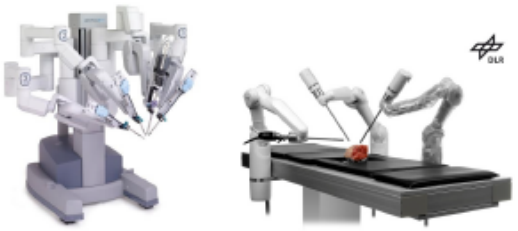

(a) da Vinci (©2011 Intuitive Surgical Inc.) (b) MiroSurge (©2011 DLR)

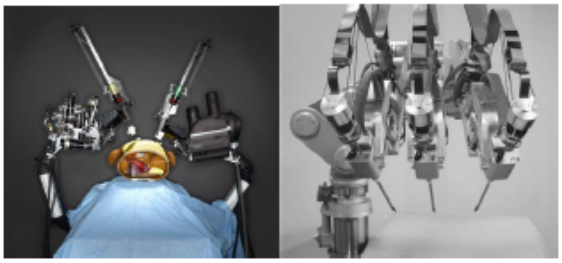

(c) RAVEN (d) SOFIE

Fig. 1: Existing research and commercially available minimally invasive robotic surgery systems

A large area of interest in robotic telesurgery is haptics: providing force feedback to the operator of a robot. One of the downsides to traditional teleoperation is that the surgeon is unable to feel the forces applied to organs or a suture. When operating traditional laparoscopic tools, the surgeon is able to directly feel how much force is being applied.

Researchers at the Technical University of Eindhoven have developed the SOFIE (Surgeon's Operating Force feedback

Daniel Jones is an undergraduate in Electrical and Computer Engineering, Worcester Polytechnic Institute (WPI), Worcester, MA 01609, USA dtjones@alum.wpi.edu

Andrew Lewis is an undergraduate in Robotics Engineering, WPI, Worcester, MA 01609, USA alewi@alum.wpi.edu

Gregory S. Fischer is with the Automation and Interventional Medicine (AIM) Laboratory in the Department of Mechanical Engineering WPI, Worcester, MA, USA gfischer@wpi.edu

†Shared first authorship.

Interface Eindhoven) robotic arm as a means of improving upon the da Vinci system. After performing field studies on robotic surgeries with the da Vinci, SOFIE was designed with the following design requirements in mind: connection to the operating table for easier set-up; additional DoFs at the instrument tip to improve organ approach; reduced system size; and reduced costs; and force feedback for reduced operating time and increased patient safety[8].

II. Design Requirements

As evidenced by the activities of other researchers, there is a lot of research still to be performed on the efficacy of haptics in MIRS. To this end, the arm was designed to be able to report information of the forces from each of the actuators. This will allow for future research to be performed on haptic feedback as well as how the forces of the arm should be mapped onto the controller. The internal and external communications for the haptic data were designed to be sufficiently fast to allow for an effective force feedback loop.

In teleoperation, there can potentially be a significant lag introduced between the surgeon and the arm and then back from the arm to the surgeon. The effects of this delay, especially when haptic feedback is incorporated, also needs to be investigated. The software for the arm was designed to allow for the arm to be easily operated over a network, as well as to allow for delays to be artificially introduced so that research on the acceptable delays could be performed.

Whether through mechanical or software means, maintaining a Remote Center of Motion (RCM) is necessary when performing any kind of laparoscopic surgery. Thus, the robot was designed to be able to maintain an RCM. Additionally, improvements upon the da Vinci and other systems were taken into consideration in the design of the StandAlone Surgical Haptic Arm (SASHA). At the head of these improvements was the ability to easily place place the robot and position its RCM in a surgical environment.

III. Design Overview

A. Manipulator Design

The first iteration of SASHA, shown in Fig. 2, is a fully functional prototype. As such, it was designed to be highly tunable and easy to manufacture. The support structure is built with sheets of laser-cut acrylic held together with tapped blocks in the vertices. Ease of manufacturing and repeatability of parts was a major factor in designing the arm. There are several locations where the timing belt tensioners can be placed, which allows for a range of possible belt tensions. Additionally, the use of acrylic makes it easy and relatively inexpensive to replace single plates or entire components as part of an iterative design cycle. As a research tool, this will be particularly useful in experimenting with the optimal workspace and ergonomics of the robot.

It was decided that mechanically coupling opposite the links of the arm would be a reliable and simple solution for maintaining an RCM; as there is ostensibly no risk of software error in maintaining the remote center and it allows for the motions of a many-sectioned arm without requiring all of the joints be actively actuated. SASHA utilizes 2 sets of timing belts at the joint axles to keep opposite links parallel. In this configuration there need only be 3 DoFs: 2 perpendicular rotations about the RCM and one linear translation through it. With only 3 degrees of freedom, the forward and inverse kinematics of the tool wrist are particularly easy to calculate, which greatly decreases the performance requirements of the high level kinematics controller. In order to keep the inertia of the arm as minimal as possible, the rotational axes are actuated by motors located in the base. These large motors are highly geared in such a fashion to allow for back drivability for positioning the arm. As a safety measure, the larger motors have an integrated elctro-mechanical brake to keep the position of the arm in the unlikely case of loss of power. The linear actuation requires much less power compared to the other motions, thus these smaller motors are located on the same link as the da Vinci tool manipulating carriage.

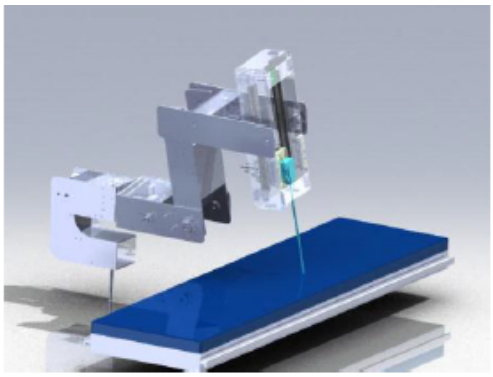

Fig. 2: Computer rendering of functional StandAlone Surgical Haptic Arm (SASHA) prototype. The arm maintains an RCM at the surgical point of entry and provides 3 positional degrees of freedom in addition to the 4 manipulating DoFs provided by the da Vinci tool.

The standard tool manipulating carriage interfaces directly with the standard da Vinci tool faceplate, which holds and interacts with the tool. As with the da Vinci system, each of the driving discs is individually spring-loaded; allowing for reliable, positive interaction with the tool interface. The levers on the sides of the tool allow for release from the interface. Custom torque sensors are placed between the motor and the tool in each spring-loaded module as seen in Fig. 3.

The ability to easily position the robot is especially important with a robot with a mechanically fixed RCM, as it must be placed in the correct place and orientation. Positioning of the arm is currently passive in four axes: along the length of the operating table support rail, two rotations about the support rail mount and a linear translation through the mount. The rail mount is provided by Allen Medical Systems and supports a stainless steel rod that can be positioned and then easily secured. The next step in improving the positioning

Fig. 3: Torque sensor and spring-loaded tool interface. The interface interacts directly with the standard da Vinci faceplate and is capable of manipulating the tool wrist while measuring the forces being applied to the tool tip.

Fig. 4: First prototype of SASHA Research Platform, showing the da Vinci tool, links of the arm, and tool manipulation motors

of the robot is implementing the ability to position SASHA along an axis parallel to the operating table support rail. step in improving the positioning of the robot is using another link with 2 passive rotations.

B. Electrical Design

The electronics for this arm need to be able to provide precise control of each degree of freedom, and also provide force feedback to the user. The arm also needs to be able to operate over long distances or have the option to insert delays to facilitate research into teleoperation and haptics. This system is outlined in Fig. 5. The user interface is a PHANTOM desktop from Sensable, interfaced to a PC. This is connected to another program in the same or a different PC, which serves as the master for the other components. This controller talks to the remaining boards over RS485. Each motor is controlled by an individual motor controller which runs speed, position, and current control loop internally. A 24 Volt 40 Amp power supply is used to power the motor controllers and the force sensor interface. The use of RS485 and a single voltage supply means that only four wires total needed to be run to the motor controllers and the force decoder, greatly simplifying wiring within the arm.

Brushed DC motors with integral encoders are used to drive the arm. These motors need to be controlled at precise

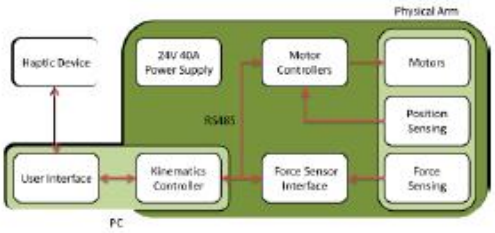

Fig. 5: System block diagram. In future experiments, articial time delays will be introduced between the User Interface and the Kinematics Controller.

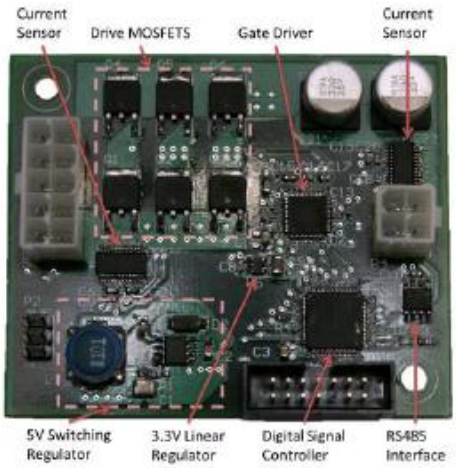

Fig. 6: 20 Amp arm motor control board with current sensing and brake control

speed and positions. It was also required that the motor controllers report forces back to the operator at rates sufficient for haptics. To this end, custom motor controllers were designed to communicate over a multidrop RS485 connection at 3 Mbaud, allowing them to report back their respective forces at greater than the 1kHz necessary for hard surface haptic rendering[9].

Two different types of motors were used, with two high power motors on the arm, two small motors on the linear slide, and four more of the small motors on the tool manipulator. The two high power motors also have electromagnetically released brakes, allowing for the gross positioning of the arm to be locked in place. The controller for the high power motors can be seen in Fig. 6 and the controller for the low power motors can be seen on the left in Fig. 7. Each of these motors has a quadrature encoder attached, and additional optical switches allow for homing. Each of the motor controllers also has on board current sensing, allowing for torque to be estimated, controlled, and reported back over RS485.

Each of the motor controllers uses an H-bridge switched using pulse width modulation to allow for the motors to be controlled with variable speed. The low power motor

controller uses an single IC with an internal H-bridge to drive the motors at up to 1 amp and 24 volts. The high power motor controllers use discrete MOSFETs in an H-bridge with a three phase gate driver. The high power board actually includes three half H-bridges, with two used to control the motor and one used to control the brake. This board is capable of driving a motor at 20 amps and 24 volts.

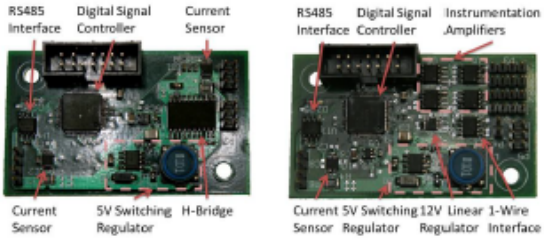

Fig. 7: Tool manipulation motor control board and torque sensor interface board with 1-Wire da Vinci tool interface

The torque sensors discussed earlier consist of 4 strain gages on a semi-deformable machined aluminum piece. The strain gages are placed in a full Wheatstone bridge configuration with an instrumentation amplifier to provide a signal that can be used in haptic rendering. In this configuration it should be possible to measure up to .6 Nm at each tool driving disc. It was decided to measure the tool torques in this manner because it does not require modifying the tool and does not rely on potentially variable motor characteristics. However, this method does not isolate the forces on the tool tip from such factors as stretch in the cables or deflection of the tool shaft. It is proposed that these intermediate forces will not interfere significantly or disproportionally enough to affect the haptic feedback.

A board was designed (Fig. 7), that can read the strain gages seen in Fig. 3 using instrumentation amplifiers and report the forces back over the RS485 connection. The da Vinci tools also have identifying information stored regarding their specific functionality, which is accessed using a 1-wire protocol from Maxim. The sensor board reports the identifying information via RS485 after retrieving it using a 1-wire interface circuit. The layout of the Faulhaber motor control boards and most of the components not specifically used to drive the motor were reused in creating this sensor board. This greatly cut down on the time taken to develop the sensor board and allowed for many of the same parts to be used on both boards.

C. Software

Each motor controller runs software written in C to handle the position and velocity control of the motors, as well as fault detection. These commands are received over the RS485 connection and feedback is sent over the same connection. Each of these motor controllers is running PID control loops on speed, position, and current.

A USB to RS485 converter was used to connect a PC to the motor controllers and the sensor board. A Java program running on the PC performs all of the kinematics calculations while also mapping the forces and movements to and from the haptic controller. A link over TCP/IP connects this to either a separate PC or another process on the same PC which interfaces to the haptic controller. A PHANTOM Desktop haptic controller from Sensable is used as the controller for the arm. The PHANTOM has 6 DoFs, which is sufficient to position and orient the tool tip, however not enough to inherently control the gripping action. A well defined API will allow for the arm to easily be interfaced to by other software. Decoupling the kinematics of the system is particularly easy: the position of the wrist is controlled by the major axes of the arm, and the orientation of the tool is controlled entirely by the motors on the carriage and represented by the orientation of the PHANTOM pen.

IV. Discussion

The design of the arm is finished and it is currently being assembled. Software is also being developed for both the motor control boards and for the kinematics controller. Once these have been completed, the arm will be able to manipulate the da Vinci tools about a remote center of motion. This will then be able to interface to the PHANTOM, allowing easy control of the arm. Force feedback will then also be provided through the PHANTOM.

This system will be used for research into the use of haptics in surgery, telesurgery, and as a complement to the da Vinci in performing surgeries. When an appropriate size of the system has been determined, a more permanent and sturdy construction method will be used. Furthermore, a system of laser-pointers will be used to easily and clearly locate SASHA's remote center of motion on the patient during initial set-up.

References

[1] Intuitive Surgical, "Intuitive Surgical Company Profile," 2010.
[2] Intuitive Surgical, "The da Vinci Surgical System," 2010.
[3] Institute of Robotics and Mechatronics, "MiroSurge - Telemanipulation in minimally invasive surgery," 2010.
[4] A. R. L. et al., "Robotic Surgery: A Current Perspective," tech. rep., Department of Mechanical Engineering, Drexel Unviersity and Drexel University College of Medicine, 2003.
[5] Institute of Robotics and Mechatronics, "MIRO / KineMedic," 2010.
[6] Force Dimension, "Force Dimension Website," 2011.
[7] B. H. et al., "Evaluation of RAVEN Surgical Telerobot during the NASA Extreme Environment Mission Operations (NEEMO) 12 Mission," tech. rep., Department of Electrical Engineering, Unviersity of Washington, 2009.
[8] L. van den Bedem, N. Rosielle, and M. Steinbuch, "Design of slave robot for laparoscopic and thoracoscopic surgery," in *20th International Conference for Medical Innovation and Technology*, 2008.
[9] B. Hannaford and A. M. Okamura, *Springer Handbook of Robotics*, ch. 30. Haptics. Springer, 2008.